

**Design and Analysis of donor-acceptor-donor parts of Organic materials for  
Photovoltaic Cells**



**By**

**Ahmad Mujtaba**

**00000326117**

**Supervisor**

**Dr. Uzma Habib**

**MS Computational Science and Engineering  
School of Interdisciplinary Engineering and Sciences (SINES)  
National University of Sciences and Technology (NUST)  
Islamabad, Pakistan**

**2024**

Design and Analysis of donor-acceptor-donor parts of Organic materials for  
Photovoltaic Cells

By

Ahmad Mujtaba

00000326117

Supervisor

Dr. Uzma Habib

A thesis submitted in partial fulfillment of the requirement for the degree of  
Master of Science

in

Computational Science and Engineering

School of Interdisciplinary Engineering and Sciences (SINES)

National University of Sciences and Technology (NUST)

Islamabad, Pakistan

2024

### THESIS ACCEPTANCE CERTIFICATE

Certified that final copy of MS/MPhil thesis written by Mr. Ahmad Mujtaba Registration No. 00000326117 of SINES has been vetted by undersigned, found complete in all aspects as per NUST Statutes/Regulations, is free of plagiarism, errors, and mistakes and is accepted as partial fulfillment for award of MS/MPhil degree. It is further certified that necessary amendments as pointed out by GEC members of the scholar have also been incorporated in the said thesis.

Signature with stamp: \_\_\_\_\_

*Uzma*  
Dr. Uzma Habib  
Associate Professor  
SINES - NUST, Sector H-12  
Islamabad

Name of Supervisor: Dr. Uzma Habib

Date: 05-01-2024

Signature of HoD with stamp: \_\_\_\_\_

*Fouzia*

Dr. Fouzia Malik  
HoD Sciences  
Professor  
SINES NUST Sector H-12  
Islamabad

Date: 8-01-2024

### Countersign by

Signature (Dean/Principal): \_\_\_\_\_

*H. d.*  
*H. a.*

Date: \_\_\_\_\_

12/01/2024

## **Declaration**

I affirm that my thesis work, titled "Design and Analysis of *Donor-Acceptor-Donor Components of Organic Materials for Photovoltaic Cells*," was conducted under the supervision of Dr. Uzma Habib at the School of Interdisciplinary Engineering and Science (SINES) within the National University of Sciences and Technology (NUST). I hereby declare that, to the best of my knowledge, this work is entirely original and does not contain any material that has been submitted for the award of other degrees in my name at any other university. Additionally, I confirm that no previously published or written material by any other individual has been included in this thesis, except where proper references have been provided for previously published works.

**Ahmad Mujtaba**  
MS Computational Science & Engineering

## **STATEMENT OF ORIGINALITY**

With this statement, I hereby declare that the submitted Master's thesis is, to the best of my knowledge, my own original work. I certify that the intellectual content of this thesis is the result of my own hard work and that all the assistance received in preparing this thesis and sources have been acknowledged.

**Ahmad Mujtaba**

*Dedicated to my exceptional parents and my wife and my  
brother & sisters whose tremendous support and cooperation  
led me to this wonderful accomplishment...*

## Acknowledgment

*Recite in the name of Lord who created- Created man from a clinging substance. Recite and your Lord is the Most Generous – Who taught by the pen – Taught man which he knew not.”*  
(Sura Al-Alaq)

I am extremely thankful to the Almighty **Allah**, the Most merciful, for providing me with the ability, understanding, and guidance to complete this research study as a requirement for my master’s degree. I would acknowledge that’s this work has never been completed without the blessing and belief of Allah and the guidance of the holy prophet **Muhammad SAW**.

I am ever so grateful to my advisor, **Dr. Uzma Habib**, for her outstanding support, insightful guidance, and, most importantly, for believing in me. I acknowledge her significant contribution to not only my research but professional growth as well. Her immense knowledge, experience, and leadership have made my journey very productive and progressive.

I am also grateful to the NUST and SINES department for providing us the facilities and opportunities which has further accelerated my passion to pursue my research. I would like to thanks the IESE department for facilitating me in completing the experimental work.

I pay special thanks and gratitude to my parents, wife and my brother and sisters for their constant support, prayers, and encouragement in my successful academic journey.

I heartily acknowledge that I am blessed to be surrounded by such wonderful people and being part of the NUST, in my life, this accomplishment would not have been possible without them.

Thank You.

# Table of Contents

<b>Chapter 1 Introduction</b> .....	1
1.1 Background of Solar Photovoltaic Cells .....	2
1.2 Structure of PV cells .....	3
1.2.1 Semiconductor layers .....	3
1.2.2 Conducting materials .....	4
1.2.3 Anti-reflecting coating .....	4
1.3 Mechanism .....	5
1.4 Materials .....	6
1.4.1 Thin film solar cells .....	7
1.4.2 Crystalline Silicon .....	11
1.4.3 Polymer solar cell .....	13
1.4.4 Hybrid solar cells .....	13
1.4.5 Dye-sensitized solar cells .....	14
1.5 Why Organic materials are preferable? .....	15
1.6 Different Organic Solar Cell Device Architectures .....	16
1.6.1 Single Layer Organic Solar Cell .....	17
1.6.2 Double Layer Organic Solar Cell .....	18
1.6.3 Bulk heterojunction (BHJ) organic solar cell .....	18
1.7 Materials for OPV .....	19
1.7.1 Electron-donor materials .....	20
1.7.2 Electron-acceptor materials .....	21
1.7.3 Donor-acceptor polymer .....	22
1.7.4 Electron donor-acceptor-donor (D-A-D) .....	23
1.8 Computational Studies .....	23
1.8.1 Classical Mechanical Methods .....	24
1.8.2 Quantum Mechanical Methods .....	25
<b>Chapter 2 Literature Review</b> .....	29
2.1 History of Photovoltaics .....	29
2.2 Organic Photovoltaic cells .....	31
2.3 Organic Materials in PV cells .....	31

2.3.1	Donor Materials .....	31
2.3.2	Acceptor Materials.....	33
2.3.3	Donor-Acceptor materials.....	35
2.3.4	Donor-Acceptor-Donor.....	38
<b>Chapter 3 Methodology .....</b>		<b>42</b>
3.1	Molecular Modelling.....	43
3.1.1	GaussView06 .....	43
3.1.2	Gaussian-09.....	44
3.2	Density functional theory (DFT).....	45
3.2.1	Geometry Optimization .....	46
3.2.2	Frequency calculations.....	47
3.2.3	Molden .....	47
<b>Chapter 4 Results.....</b>		<b>48</b>
4.1	Molecular Modeling.....	48
4.2	Geometry optimization.....	50
4.3	HOMO-LUMO Energy Gap .....	54
4.4	Electronic properties .....	55
4.5	Electronic Transition and Absorption spectra.....	56
4.6	Photovoltaic properties.....	59
<b>Chapter 5 Discussion .....</b>		<b>67</b>
<b>Chapter 6 Conclusion .....</b>		<b>67</b>
<b>Future perspective.....</b>		<b>69</b>
<b>References .....</b>		<b>70</b>

# List of Figures

<b>Figure 1.1:</b> Primary components of a PV cell [20] .....	4
<b>Figure 1.2:</b> Simple mechanism of PV cells [22] .....	5
<b>Figure 1.3:</b> PV materials [1]. .....	6
<b>Figure 1.4:</b> Thin-film and crystalline silicon solar module annual production capacity [24] .....	7
<b>Figure 1.5:</b> Hybrid Solar cell .....	14
<b>Figure 1.6:</b> Principle of dye-sensitized solar cell.....	15
<b>Figure 1.7:</b> Single Layer Organic Solar Cell .....	17
<b>Figure 1.8:</b> Double Layer Organic Solar Cell.....	18
<b>Figure 1.9:</b> Bulk heterojunction (BHJ) .....	19
<b>Figure 1.10:</b> Some examples of electron-donor materials .....	21
<b>Figure 1.11:</b> Some examples of electron-acceptor materials .....	22
<b>Figure 2.1:</b> Overview of the oil price.....	30
<b>Figure 2.2:</b> Some examples donor-acceptor polymers.....	36
<b>Figure 3.1:</b> Methodology Flow chart of Computational Modelling .....	42
<b>Figure 3.2:</b> Molden: a graphical visualization tool.....	46
<b>Figure 4.1:</b> General structure of Pristine molecule .....	49
<b>Figure 4.2:</b> Structural representation of molecules (M1-M8) using ChemDraw Ultra 12.0 .....	50
<b>Figure 4.3:</b> Optimized Structure of Pristine molecule .....	51
<b>Figure 4.4:</b> Optimized geometries of M1-M4 using B3LYP/6-31G(d) level of DFT. ....	52
<b>Figure 4.5:</b> Optimized geometries of M5-M8 using B3LYP/6-31G(d) level of DFT .....	53
<b>Figure 4.6:</b> The Graphical representation UV-Vis spectrum of Of M1-M8.....	59
<b>Figure 4.7:</b> The Graphical representation of Voc (eV) and $\alpha$ (eV) of Mol-1 to Mol-8.....	69

## List of Tables

**Table 2.1.** Different types of organic materials, and their reported efficiency ranges in the literature.

**Table 4.1:**The Energy value of Optimized geometries of M1-M8 in eV ..... 53

**Table 4.2:** HOMO-LUMO energy values and Energy gap values of Pristine and M1-M8 ..... 54

**Table 4.3:** HOMO-LUMO energy values and Energy gap values of Pristine and M1-M8 ..... 55

**Table 4.4:** The absorption  $\lambda_{\max}$  (nm), oscillator strength (O.S), of Pristine and M1-M8 ..... 56

**Table 4.5:**Theoretical absorption  $\lambda_{\max}$  (nm), vertical excitation energy  $E_{tr}$  (eV), oscillator strength (O.S), and (MO/character) of M1-M8 optimized geometries ..... 58

**Table 4.6:** Showing the relationship of HOMO, LUMO, energy gap,  $V_{oc}$  and  $\alpha$  of M1-M8 ..... 60

**Table 4.7:** Energy Gap Values Pristine and Mol1-Mol8 ..... 63

## List of Abbreviations

OSCs	.....	Organic solar cells
PV	.....	Photovoltaic
CdTe	.....	Cadmium telluride
CIGS	.....	Copper Indium Gallium Selenide
GaAs	.....	Gallium arsenide
PSC	.....	Polymer solar cell
DSSCs	.....	Dye-sensitized solar cells
OPV	.....	Organic photovoltaic
$E_g$	.....	Bandgap
DFT	.....	Density functional theory
MD	.....	Molecular Dynamics
HOMO	.....	Highest occupied molecular orbital
LUMO	.....	Lowest unoccupied molecular orbital
O.S	.....	Oscillator strength
Voc	.....	Open circuit voltage

## Abstract

The conversion of solar energy into electrical energy using photovoltaic cells is currently one of the most exciting research challenges. Organic photovoltaic (OPV) cells are in high demand for photovoltaic applications because of their mechanical flexibility, affordability, ease of production, and lightweight nature. The research has primarily focused on D-A-D (Donor-Acceptor-Donor) photovoltaic cells, extensively investigating the nature of Donor 1, Acceptor, and Donor 2 units. It has been observed that attaching carbon chains to both the Donor and Acceptor units can have positive effects on the efficiency of these organic photovoltaic material. The effect of carbon chain that bridges the D-A and A-D has not been investigated in literature. Therefore, in this research computational analysis was conducted on the organic materials for OPV utilizing quantum chemical calculations based on density functional theory (DFT) with the B3LYP hybrid functional and the 6-31G(d) basis set. The carbon chain length between donor-acceptor and acceptor-donor part of pristine organic materials was investigated for use in organic photovoltaic cells. A comprehensive investigation is performed to compare the relative energies, electronic characteristics, molecular orbital properties, absorption spectra, and photovoltaic qualities. According to the computed data, it has been observed that the relative energy increases with the addition of one or more methyl groups between the Donor-1 and Acceptor part or Acceptor and Donor-2 part of pristine molecule. The HOMO-LUMO of modeled structures has almost the same energy gap is  $\sim 0.22$  eV like the pristine structure. The absorption data shows the increase in  $\lambda_{\text{max}}$  with the addition of four carbon atoms but the photovoltaic properties,  $V_{\text{oc}}$  (open-circuit voltage), is decreased from 0.60 to 0.51. It is concluded that the length of carbon chain length between the donor-acceptor and acceptor- donor units of D-A-D organic material has no significant impact on the efficiency of the photovoltaic cell.

# Chapter 1

## Introduction

Solar energy is widely recognized as a plentiful and environmentally friendly form of power, prompting researchers to devote considerable resources towards its use in the production of electricity. [1] One popular method is photovoltaics, which utilize the photovoltaic effect to convert solar energy into electricity. Photovoltaics can be classified into two distinct categories: inorganic and organic. Significant advancements have been made in the field of inorganic solar cells over the course of the past several decades. [2]. An important step forward was taken in 1954 when Bell Labs developed the initial silicon-based (inorganic) solar cell. [3]. The PCE of silicon solar cells has increased from 5% to 25% in that time. [4]. Despite these advancements, inorganic photovoltaic cells still have a number of significant limitations, including expensive materials, environmental toxicity, bulky panels, a high initial investment for commercialization, and complicated production procedures [2].

Organic solar cells (OSCs) in contrast to their inorganic counterparts have several benefits. As they can be created using affordable materials and simple production techniques, their cost-effectiveness is one of their most significant advantages. The flexibility, robustness, and lightweight nature of OSCs are further characteristics. In organic solar cells, the photoactive layer is often composed of conducting polymers or extremely small organic molecules. These materials also have the advantage of being precisely tailored by synthetic alterations, which improves their capacity to match the entire solar spectrum's absorption range.

In the initial stages of study on organic photovoltaics, the original focus was on simulating the light-harvesting capacities of chlorophyll and utilizing them in solar cells due to their effective light absorption features [5]. The creation of new light-absorbing molecular and polymeric materials propelled the improvement of organic solar cell (OSC) technology as research went on [6-9]. During the 1980s, researchers successfully produced a solar cell based on polymers, which had a power conversion efficiency of 0.1% or lower. [10]. Later, in 1995, Professor Alan Heeger presented the idea of a bulk heterojunction (BHJ), which significantly accelerated the development of OSC research[11].

### **1.1 Background of Solar Photovoltaic Cells**

Practical applications of renewable energy sources, especially solar energy, have increased steadily since the 1970s, when the world was gripped by an oil crisis. There is a pressing need to maximize the use of solar power. has prompted scientists and policymakers worldwide to priorities the development of more efficient and effective methods, particularly in the field of propulsion. Solar energy can be harnessed in terrestrial regions in one of two unique ways: the first is the sun thermal route, which involves the utilization of solar heaters ,collectors, dryers, and other devices of a similar kind; the second is the solar electrical route, which involves the utilization of solar photovoltaic systems.[12].

The photovoltaic process converts sunlight directly into electricity and does not require the involvement of any intermediaries. Solar photovoltaic (PV) systems can generate anywhere from a few hundred milliwatts to several megawatts of power on their own, and they have several advantages over traditional power sources. The significance of the autonomous photovoltaic (PV) system in facilitating the provision of electricity to rural regions, particularly within developing nations, has been of paramount importance. When a solar photovoltaic module is combined with

a battery system and a charge controller, the result is a solar home lighting system, which is a complete way to power homes in rural areas. This has led to more people wanting to use solar PV technology for different things, which has raised demand. [13-16].

PV cells made considerable advancements and obtained useful uses in the 1950s. Bell Labs invented high-power silicon photovoltaic cells in 1954. This solar cell could convert 6% of sunlight into energy. The evolution of solar technology was advanced by this remarkable achievement. [17]. The US Vanguard I satellite initially used a PV array-powered radio in 1958, making it the first commercial application of the technology. However, each had its limitations. Other PV cell materials like cadmium telluride, gallium arsenide, indium phosphide and cadmium sulphide were also investigated. Silicon photovoltaic (PV) cells, because of their benefits, were considered the most promising technology [18].

### **1.2 Structure of PV cells**

Photovoltaic (PV) cells, commonly known as solar cells, are specialized devices designed to convert sunlight into electrical energy by harnessing the photovoltaic effect. PV cells are the most basic portion of PV systems [19]. The main components of a solar PV cell include (Figure 1.2):

- Semiconductor layers
- Conducting materials
- Anti-reflecting coating

#### **1.2.1 Semiconductor layers**

The semiconductor layer, also known as the absorber or active layer, is crucial in a solar cell as it efficiently absorbs and converts sunlight into electrical current through the photovoltaic effect. Solar cells are composed of two distinct semiconductor layers: The N-type semiconductor layer,

also known as the emitter, and the P-type semiconductor layer, referred to as the base. These two layers are sandwiched and hence there is formation of P-N junction.

### **1.2.2 Conducting materials**

A conductive material, frequently a thin metal layer, is positioned above the semiconductor layer. This layer facilitates the passage of electron-hole pairs to exit the solar cell. Solar cells lacking a conductive material on their upper surface are incapable of producing an electric current.

### **1.2.3 Anti-reflecting coating**

The efficiency of the solar cell is improved by applying an anti-reflective coating to its front side. Because this coating lowers light reflection, more photons can reach the semiconductor materials. A solar cell without an anti-reflection layer would reflect light, not excite electrons.

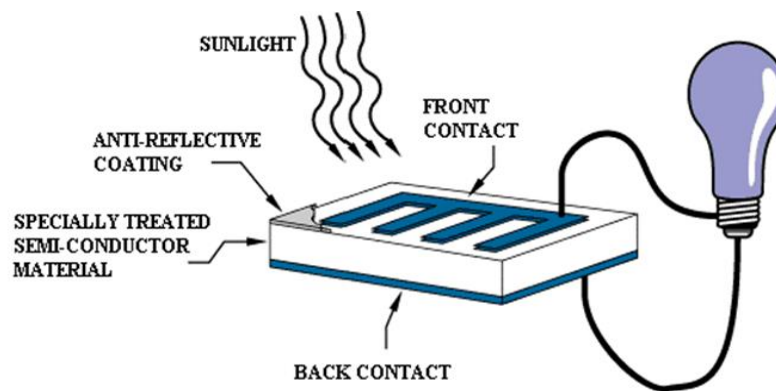


Figure 1.1. Primary components of a PV cell [20]

### 1.3 Mechanism

The solar cell mechanism operates on the principle of the photovoltaic effect, wherein sunlight is directly converted into electrical energy. Solar cells, predominantly composed of semiconductor materials like silicon, possess distinctive characteristics that enable the generation of an electric current upon exposure to sunlight. [21]. The mechanism of a photovoltaic (PV) cell involves several steps. Here is a simplified explanation of the PV mechanism.

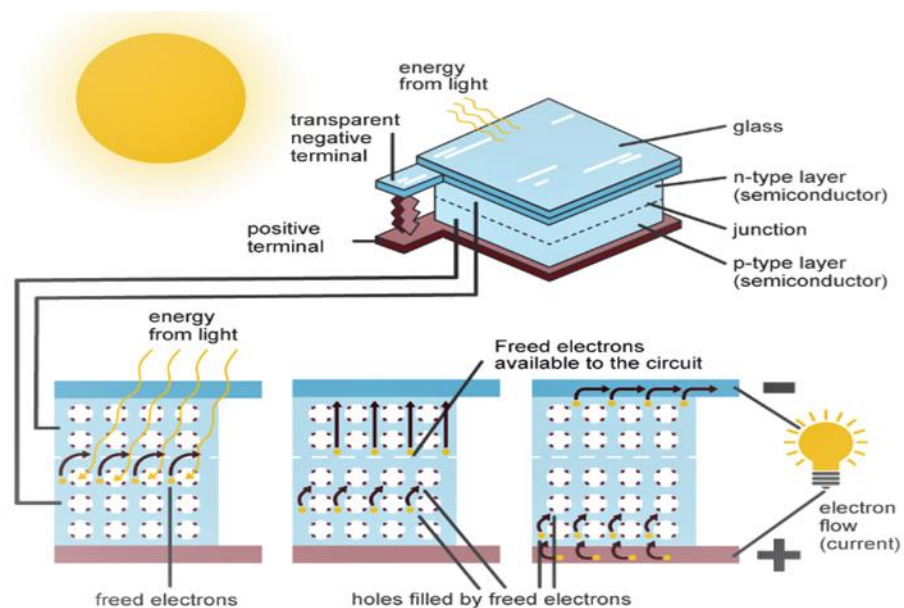


Figure 1.2. Simple mechanism of PV cells [22]

A solar cell is fabricated using two distinct categories of semiconductors, namely n-type and p-type semiconductors. The uppermost layer, known as the N-type layer, exhibits a very small thickness and is characterized by a significant abundance of electrons. (Figure 1.1). The lowermost layer, referred to as the P-type layer, exhibits a significant abundance of holes. These two layers are sandwiched and hence there is formation of P-N junction, the electrons in the N-type semiconductor exhibit a tendency to migrate towards the P-region, so establishing a layer of negative charge. Conversely, the holes in the P-type semiconductor manifest a desire to move

towards the N-region, resulting in the formation of a positive charge layer. The depletion area is situated within the semiconductor, sandwiched between its two layers. When sunlight goes through the thin top layer, it is easy for it to reach this depletion region, which has neutral atoms and no charge. These neutral atoms split apart when photons from the sun encounter the depletion layer. Neutral atoms lose electrons, creating holes for free charge carriers. Holes in the depletion area cause electrons to go towards N-type and holes to move towards P-type. When an electronic circuit is connected, an electron passes through, creating power for electrical appliances like lights and fans, among others.

### 1.4 Materials

There are numerous varieties of photovoltaic materials that can be used to construct solar cells as shown in Fig.1.2 [23].

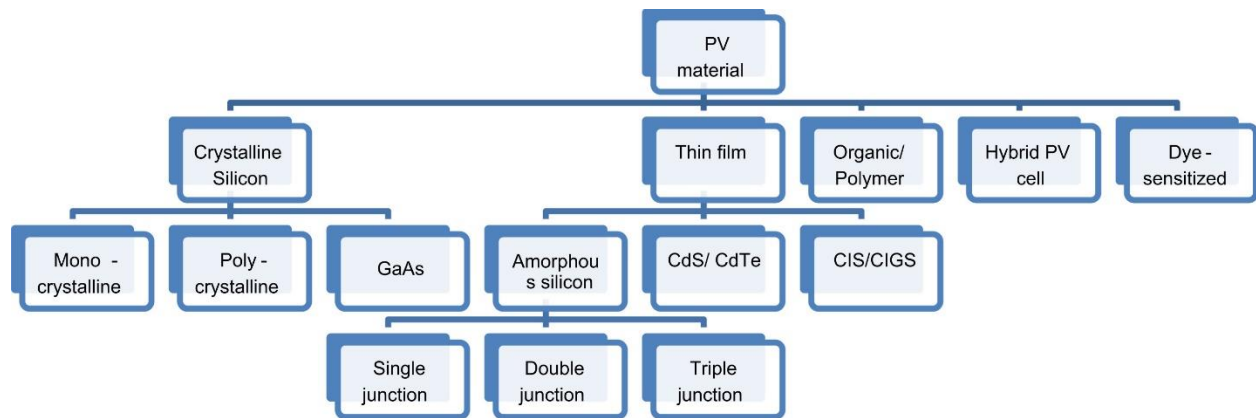


Figure 1.3. PV materials [1].

However, as can be seen in Fig. 1.3 [24], Solar cells based on silicon hold a dominant position in the market owing to their well-established technology and impressive efficiency levels. This has led to a continuous rise in the global manufacturing of PV cells and modules throughout time. Crystalline semiconductors, such as silicon and gallium arsenide, offer the highest level of efficiency when compared to the alternatives available on the market. Solar cells that are made

from materials that are not as pure as others, such as amorphous inorganic or organic materials, polycrystalline, or a mix of these, have a poorer performance, but they are also less expensive. [25]. Therefore, scientists are looking into more effective alternatives to using solar cells to generate electricity all around the world. The technology of thin films has been viewed as a possible technology because it is less expensive and lighter than mono- and poly-crystalline solar cells, but the scientific community is still concerned about its low efficiency [26]. Researchers throughout the world are studying amorphous silicon, CIS and CdS/CdTe, in an effort to improve the performance of thin film technology. [27]. However, the utilization of polymers and organic material-based films processes emerges as feasible alternatives due to the environmental concerns connected with conventional materials. [28]. The following solar cell material research advances are listed below:

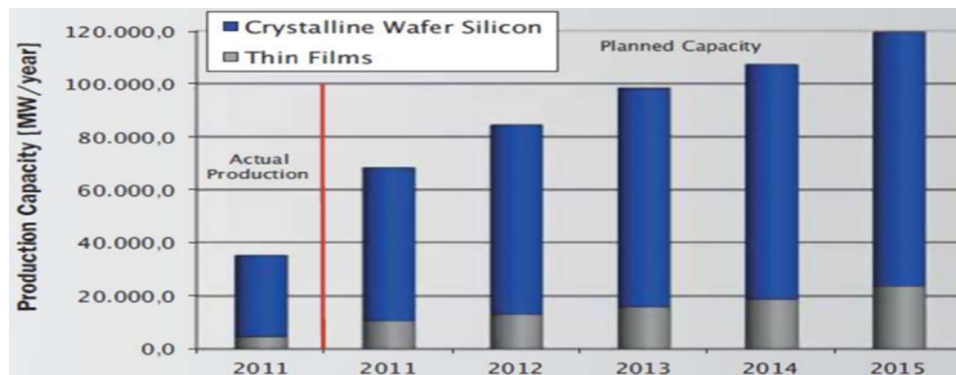


Figure 1.4. Thin-film and crystalline silicon solar module annual production capacity [24]

### 1.4.1 Thin film solar cells

Thin-film solar cells are a type of photovoltaic cells that exhibit a lighter weight and enhanced flexibility compared to conventional silicon-based solar cells. Thin layers of semiconductor materials are layered onto a supporting substrate comprised of materials that consist of glass, plastic or metal rather than requiring thick wafers of silicon to construct them. Solar cells made

with thin film technology are more cost-effective than those made with silicon since the former requires less material in the manufacturing process[28]. Thin film solar cells are categorized based on the materials employed in their photovoltaic (PV) layers, with the primary classifications including:

- Cadmium telluride
- Amorphous silicon
- Copper indium gallium selenide

### **1.4.1.1 Cadmium Telluride**

Cadmium telluride (CdTe) is a crystalline compound semiconductor that exhibits a high level of efficiency and facilitates light absorption due to its characteristic straight band gap. Typically, the p-n junction diode is fabricated by sandwiching cadmium sulphide layers between two semiconductor layers. [34]. Cadmium telluride (CdTe) is a popular choice for making photovoltaic (PV) systems that are cheaper and more economically viable, as well as the first low-cost PV technology [35, 36]. Cadmium telluride (CdTe) possesses a band gap of 1.5 electron volts (eV), demonstrating a high level of optical absorption efficiency and exhibiting remarkable chemical stability. Due to its inherent characteristics, CdTe exhibits significant potential as a preferred material for the fabrication of thin-film solar cells. As a result, its efficiency typically ranges between 9% - 11% [35, 37]. Cadmium in solar cells presents serious problems for the environment. Cadmium is a heavy metal that may quickly build up in people, animals, and plants. It is also hazardous. It is expensive to properly dispose of and recycle cadmium-based products, and doing so could have negative effects on society and the environment [38, 39]. Therefore, the main problems with this CdTe technologies are the limited availability of cadmium and an associated environmental risk.

### **1.4.1.2 Amorphous silicon**

Amorphous silicon PV modules were among the first industrially made solar cells. In the manufacturing of a-Si solar cells, low processing temperatures allow the use of inexpensive materials like polymer and other substrates that are flexible. These substrates take less energy to process, which contributes to the manufacturing process's overall energy efficiency [29]. Amorphous silicon, characterized by its non-crystalline and disorderly structure, exhibits a significantly higher light absorption rate, approximately forty times faster than that of monocrystalline silicon. As a result of their higher efficiency, amorphous silicon-based solar cells are more popular than alternative materials such as CIS/CIGS and CdSa/CdTe [30]. The primary issue with a-Si photovoltaic cells is that they have a low efficiency, and their performance might be unstable. The efficiency of photovoltaic (PV) modules tends to naturally decrease at the cell level. At present, the efficiency of commercial photovoltaic (PV) modules spans from 4% to 8%. These devices are well-adapted to fluctuating climatic conditions characterized by limited sunlight exposure and are capable of efficient operation even under high temperature conditions.

#### **1.4.1.2.1 Single-junction amorphous silicon**

Single-junction amorphous silicon (a-Si) solar cells are a type of thin-film solar cell. They turn sunlight into energy using a single layer of amorphous silicon as the semiconductor material. They have lower efficiency than crystalline silicon solar cells in general, but they have advantages such as greater performance in low-light environments and flexibility[31].

#### 1.4.1.2.2 Double-junction amorphous silicon

Double-junction amorphous silicon refers to a type of thin-film solar cell that comprises two layers of amorphous silicon, each possessing different bandgap energies. In contrast to single-junction cells, the utilization of two layers in the cell enables enhanced absorption of a wider range of light wavelengths, resulting in increased efficiency in the conversion of sunlight into electrical energy. [32].

#### 1.4.1.2.3 Triple-junction amorphous silicon

Triple-junction amorphous silicon refers to a type of thin-film solar cell that expands on the concept of the double-junction cell by employing three separate layers of amorphous silicon with varied bandgap energies. Each layer captures a different wavelength of light, increasing the cell's efficiency in converting sunlight radiation into electricity throughout a wider range of the solar spectrum [33]. They are frequently used in advance photovoltaic applications, like space applications, where high efficiency and lightweight qualities are critical.

#### 1.4.1.3 Copper Indium Gallium Selenide

Copper Indium Gallium Selenide (CIGS) is a semiconductor material commonly used in the production of thin-film solar cells. It is a compound made up of copper (Cu), indium (In), gallium (Ga), and selenium (Se) elements[34]. CIGS are also semiconductors with a straight band gap. Copper indium gallium selenide (CIGS) thin film solar cells exhibit a higher efficiency, around 10% to 12% more, compared to cadmium telluride (CdTe) thin film solar cells. Copper indium gallium selenide (CIGS)-based solar cell technology has emerged as a very promising thin film technology owing to its significantly enhanced efficiency and lighter weight. [35]. In recent years, CIGS, a polycrystalline semiconductor, has been acknowledged as a highly desired material due

to its excellent efficiency on a laboratory scale, which reaches approximately 20.3% [36]. However, it has limitations, including sensitivity to humidity and environmental conditions that cause degradation over time, despite its high efficiency and popularity. Furthermore, when compared to other solar cell technologies, it's a difficult and expensive manufacturing method that prevents widespread use.

## **1.4.2 Crystalline Silicon**

Crystalline silicon is widely employed as a primary material in the production of solar cells. It is well-known for its great efficiency, stability, and dependability in converting sunlight to usable energy. Crystalline silicon solar cells possess notable advantages, such as superior efficiency compared to alternative solar cell technologies, as well as a readily available supply. These attributes have prompted manufacturers to see crystalline silicon as an optimal material for the production of solar cells. [37]. There are three classifications of crystalline silicon solar cells.

- Monocrystalline Silicon
- Polycrystalline Silicon
- Gallium Arsenide (GaAs)

### **1.4.2.1 Monocrystalline Silicon**

Monocrystalline silicon solar cells represent a specific category within photovoltaic technology. made from a single crystal structure using the Czochralski technique [35, 38, 39]. During the production of monocrystalline silicon solar cells, Si crystals are sliced from large ingots. This necessitates precise processing, as the "recrystallization" step is more expensive and involves multiple processes. The efficiency of monocrystalline silicon PV cells typically falls within the range of approximately 17% to 18%. [40]. Monocrystalline PV cells are employed due to their

great efficiency, but their higher cost is still a source of worry for both the producers and the final consumers. As a result, industries are exploring alternatives, and polycrystalline solar cells emerge as a viable option due to the fact that they are less expensive than monocrystalline PV cells [41].

#### **1.4.2.2 Polycrystalline Silicon**

Polycrystalline silicon solar cells typically consist of multiple separate crystals that are fused together within a single cell structure. The production of polycrystalline silicon solar cells, which involves cooling molten silicon within a graphite mold, represents an alternative that is more advantageous financially. Polycrystalline silicon solar cells have grown in popularity and are now the most extensively used solar cell technology. They are believed to have accounted for as much as 48% of worldwide solar cell production in 2008.[42]. Different types of crystals forms are produced as molten silicon solidifies. Despite having a lower efficiency, usually between 12% to 14%, these structures are more affordable to produce than solar panels made of monocrystalline silicon [43].

#### **1.4.2.3 Gallium Arsenide (GaAs)**

Gallium arsenide (GaAs) solar cells are a type of photovoltaic (PV) cell designed to convert solar energy into electrical power. by using a semiconductor material made of gallium and arsenic. GaAs solar cells offer unique features that make them ideal for specific uses. The GaAs material is more expensive than both mono- and polycrystalline silicon-based solar cells, but it has great efficiency and lightweight characteristics. The excellent heat resistance of GaAs-based solar cells, however, makes them ideal for concentrated photovoltaic (PV) modules used in power production, hybrid functions, and applications in space [44].

### **1.4.3 Polymer solar cells**

Polymer solar cells (PSCs) are a type of solar cell technology that utilizes polymers as the active material to capture sunlight and transform it into electricity. The solar cells are frequently characterized by their flexibility, which can be attributed to the presence of a polymer substrate. The first PSC was created by Kodak Research Lab's Tang et al. [45]. A polymer solar cell (PSC) is often constructed by depositing a series of thin functional layers onto a polymer foil or ribbon. This process leads to the formation of a donor-acceptor pair, with the donor being the polymer and the acceptor being the fullerene. These photovoltaic systems absorb sunlight using a variety of materials, including organic molecules such as conjugated or conducting polymers [45]. In 2000, Shirakawa, MacDiarmid, and Heeger were awarded the Nobel prize in chemistry for their discovery of conductive polymers, which represented a novel category of polymer-based substances [46]. The photovoltaic effect is the basis for the operation of PSCs and other organic solar cells. This phenomenon includes the transmission of electromagnetic radiation, like sunshine, into electrical current, which enables the conversion of light energy into electrical energy. [47]. The first achievement of a polymer solar cell with a notable power conversion efficiency was accomplished by u et al. by the incorporation of poly[2-methoxy-5-(2'-ethylhexyloxy)-p-phenylene vinylene] (PPV) in conjunction with C60 and its many derivatives. [48].

### **1.4.4 Hybrid solar cells**

A hybrid solar cell refers to a kind of photovoltaic technology that operates by facilitating the transfer of charges at the interface of two semiconductors: one of these semiconductors is organic, while the other is inorganic. Hybrid solar cells combine the benefits of organic and inorganic semiconductors, with organic components such as light-absorbing conjugated polymers acting as donors and hole transporters within the photovoltaic system [49]. In the structure of hybrid cells,

inorganic materials play the roles of acceptors and electron transporters. The materials used in hybrid solar cells are arranged in a layered structure, which is placed between two electrodes. The back contact is made of an opaque metallic electrode, while the front side of the device allows light to enter through a semitransparent conductive material like indium tin oxide (ITO)[50].

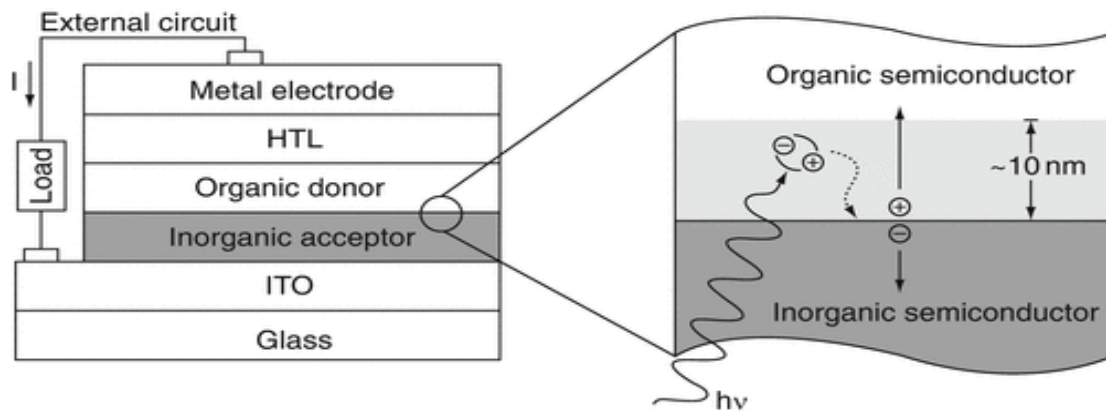


Figure 1.5. Hybrid Solar cell

#### 1.4.5 Dye-sensitized solar cells

Dye-sensitized solar cells (DS or DSSCs) are a form of thin-film solar cell that converts sunlight to electrical energy. They are also known as Grätzel cells, after their inventor [51], who created the concept in the 1990s. Dye-sensitized (DS) solar cells provide distinct benefits over silicon-based solar cells, including cost reduction and a streamlined manufacturing process. Consequently, DS solar cells present a promising alternative for forthcoming solar cell applications. In the early part of 1991 Grätzel and ORegan (52) made advancements in the field of solar energy by introducing dye-sensitized solar cells (DSSCs). The operational mechanism of these cells is shown in Figure 1.5. Solar cells that are dye-sensitized made up of numerous critical components and work on five fundamental principles. Some instances include: There is a redox mediator in the electrolyte, a sensitizing dye, a semiconductor film (e.g., TiO<sub>2</sub>), a counter electrode, and a supporting layer made of transparent conductive oxides[52]. For dye-sensitized solar cells

(DSSCs), introduced inexpensive platinum-free counter electrodes (CEs). The power conversion efficiency of the newly developed electrodes was somewhat greater compared to the dye-sensitized solar cells (DSSCs) using a traditional platinum-based counter electrode (CE), with an approximate value of 4%. The study conducted by Ahmad et al. [53].

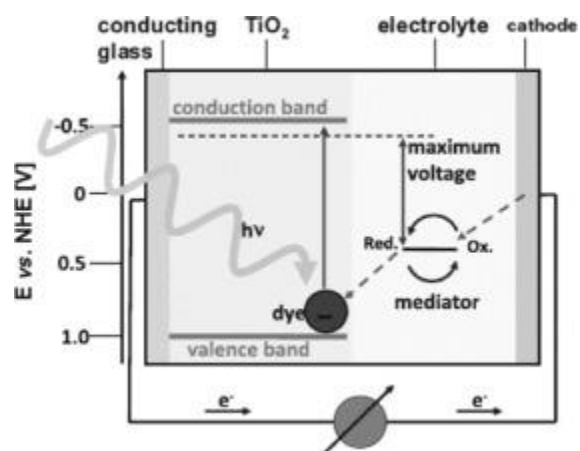


Figure 1.6. Principle of dye-sensitized solar cell

## 1.5 Why Organic materials are preferable?

Inorganic solar cell technology took a significant leap forward in 1954 with the invention of the first silicon cell by Bell Labs [38]. Significant progress in the field has facilitated the enhancement of silicon solar cells, resulting in the attainment of power conversion efficiency (PCE) levels of up to 25%. [3]. At present, most widely installed photovoltaic systems use silicon-based solar cells. Other inorganic photovoltaic systems have also had promising results in research. Sharp Monolith has created an inorganic solar cell with a 35% efficiency that is based on GaInP [54]. Inorganic solar cells also have a very long lifetime. While inorganic photovoltaics are a well-established technology, they do have their drawbacks, such as the large quantity of raw materials needed to create panels, the need for vacuum processing during manufacture, the high price of installation, and the panels' stiffness and weight[1], in addition to problems with recycling and the utilization

of limited materials, both of which render them inappropriate for certain applications[55]. New solar technologies like OPVs may fill gaps in inorganic PV. The use of scalable roll-to-roll manufacturing techniques on flexible substrates has many advantages. The cost is comparatively reduced, and the range of applications is more extensive.

Organic photovoltaics (OPVs) has garnered considerable attention in the last twenty years owing to its several benefits in comparison to inorganic solar cells. [56]. When comparing organic photovoltaic cells (OPVs) to inorganic photovoltaic cells, it can be seen that OPVs has the advantages of being lighter in weight, more cost-effective, and non-toxic in nature. They're also mechanically strong and flexible. Roll-to-roll manufacture on a big scale at a low cost allows for quick commercialization. However, the power conversion efficiency of organic solar cells is much lower than that of their inorganic counterparts. The current peak efficiency of OPVs is 13%. [57]. Stability is also a problem with OPVs because their life span is currently limited to 5000 hours, while silicon solar cells can last for 20 years. [56] As a result, the most significant goals in OPV research involve increasing power conversion efficiency and its stability.

### **1.6 Different Organic Solar Cell Device Architectures**

In organic solar cells, the typical structure is composed of three types of layers: an anode, a cathode, and an active layer. The active layer is located between the anode and the cathode. To facilitate effective charge transfer within the cell, one of the electrodes needs to be transparent to light. Indium tin oxide is commonly used as a transparent anode layer, while a metal electrode like aluminum or calcium serves as the cathode layer. Extensive research has been conducted on different device topologies for organic solar cells with the aim of enhancing charge transfer efficiency across the cell [58].

### 1.6.1 Single Layer Organic Solar Cell

A single layer organic solar cell is an organic photovoltaic device with a single layer of photoactive material sandwiched between the anode and cathode layers [10]. It improves charge generation by combining conjugated polymers with acceptor materials in the photoactive layer. The anode layer, which is often composed of indium tin oxide, lets light flow through while collecting positive charges (holes), and the cathode layer, which is typically made of metal electrode, collects negative charges (electrons). Although this architecture simplifies device manufacture, it may have difficulties in obtaining high power conversion efficiencies.

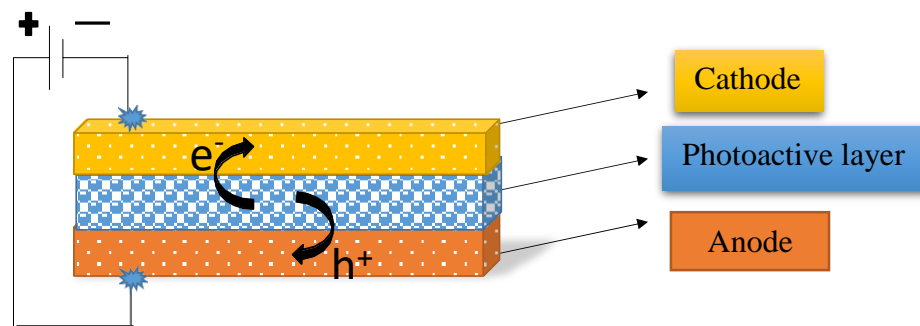


Figure1.7. Single Layer Organic Solar Cell

In single layer organic solar cell architectures, photocurrent generation relies on the work function difference between a metal electrode and an electrode. However, this design poses limitations on efficient charge carrier separation, resulting in prevalent hole-electron recombination [59]. As a consequence, these architectures suffer from low efficiency. The maximum power conversion efficiency achieved with this type of device architecture is only 0.1% [10].

### 1.6.2 Double Layer Organic Solar Cell

A double layer organic solar cell is an organic photovoltaic device with two separate layers of photoactive components. It consists of a donor layer that absorbs light and produces excitons, and an acceptor layer that efficiently separates the excitons into free charges. The double layer organic solar cell architecture typically consists of a p-type electron donor layer and an n-type electron acceptor layer. In 1986, Tang introduced this architecture, utilizing phthalocyanines as the donor layer and perylene derivatives as the acceptor layer [10].

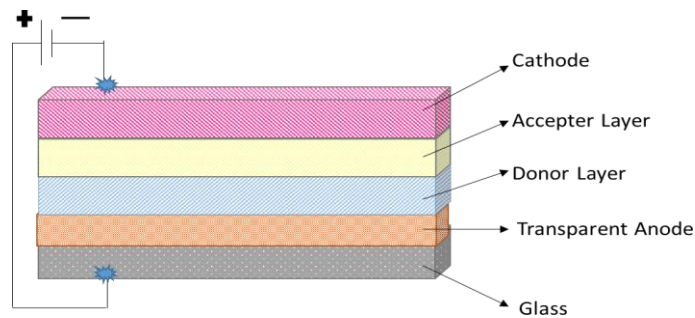


Figure 1.8. Double Layer Organic Solar Cell

In a double layer organic solar cell, charge carriers are produced when light interacts with the donor molecules. At the point where the molecules of the donor and acceptor separate, these charge carriers migrate in the direction of the electrodes with the opposite charges. The LUMO (lowest unoccupied molecular orbital) level of the donor molecule should line up with the HOMO (highest occupied molecular orbital) level of the acceptor molecule to enable this movement. The maximum power conversion efficiency achieved with this architecture has been reported as 1% [10].

### 1.6.3 Bulk heterojunction (BHJ) organic solar cell

The bulk heterojunction (BHJ) organic solar cell is a popular organic photovoltaic device architecture. The bulk heterojunction (BHJ) device architecture, proposed by Alan Heeger in 1995,

is a significant breakthrough in the field of organic solar cells [11]. A network of acceptor and donor molecules forms a network within the active layer, which is located between an anode and a cathode layer in this architecture. The larger interfacial area in the BHJ structure causes more charge carriers to be generated at the contact between the donor and acceptor molecules. This allows for efficient charge transfer between the electrodes. Conducting polymers such as poly (3-hexyl thiophene) are widely used as donors in BHJ solar cells, and fullerene derivatives as acceptors. Inverted and tandem BHJ solar cells are examples of variations on this architecture. This architecture improves charge separation by combining a transparent anode layer like indium tin oxide with a metal cathode layer. The BHJ structure has a wide interfacial area, which allows for efficient charge generation and collection, resulting in better device performance. BHJ solar cell with an architecture providing a maximum efficiency of 8.94% [11].

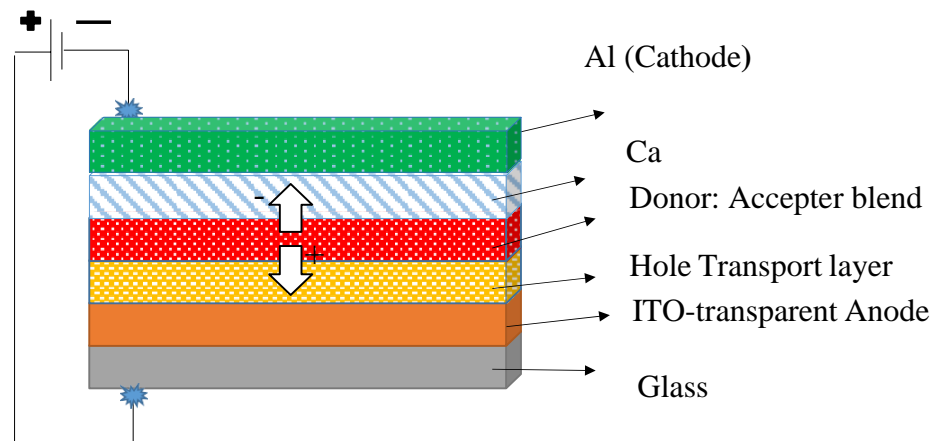


Figure 1.9. Bulk heterojunction (BHJ)

## 1.7 Materials for OPV

An Organic Photovoltaic (OPV) cell has an active layer made of thin film organic semiconductor (OS) materials such as polymers or oligomers. This active layer is sandwiched between a transparent and a metal electrode. Organic semiconductors often have either electron-donating or

electron-accepting characteristics. The materials with electron-donating properties are called electron-donor materials, and materials with electron-accepting properties are termed electron-acceptor material. The active layer in organic photovoltaic (OPV) systems is made up of a combination of electron-donor and electron-acceptor elements. Fullerene is an electron-acceptor material, whereas copper phthalocyanines (CuPc) is an electron-donor substance. As the active layer of OPV devices, contains a blend of organic semiconductor materials that act as both electron donors and acceptors [60-63]

### **1.7.1 Electron-donor materials**

Electron donor materials are compounds that can release or give electrons during chemical or physical processes. Phthalocyanines and their derivatives are among the most studied OS materials in the field of organic electronics. Their outstanding photo physical and electrochemical capabilities have led to their use as electron-donor or acceptor compounds in multicomponent systems for energy and charge transfer processes. Phthalocyanines are most frequently used as the donor units in these photoactive molecules because of their excellent light-harvesting abilities [64-66]. CuPc (copper phthalocyanines) and ZnPc (zinc phthalocyanines) are widely used metal-phthalocyanines compounds in Organic Photovoltaic (OPV) devices, primarily serving as hole transporting materials and dominant absorption materials as donor. Xue et al. conducted a study where they achieved an efficiency of around 4% under 4 suns simulated AM1.5G illumination in a double-heterojunction thin film cell (CuPc/C60), with Ag serving as the metal cathode [67]. Their continued work on (CuPc)/C60 cells with hybrid planar-mixed molecular heterojunctions has significantly boosted the efficiency to a remarkable 5.5% [67]. Sub phthalocyanines have garnered significant interest due to their unique chemistry and photo physical properties as the lowest homologues of phthalocyanines [68, 69]. According to Kristin et al.'s research [70], greater

energy level alignment and a larger open circuit voltage ( $V_{oc}$ ) make SubPc-based organic photovoltaic systems work better than other phthalocyanines-based ones. As a result, the SubPc/C60 cell is more efficient than the CuPc/C60 cell. Porphyrins and their derivatives, along with other oligomer organic materials, have been shown to be successful electron-donors [71-73]. Nevertheless, their drawback lies in their limited compatibility with flexible electronics. A variety of polymer electron-donor materials have been successfully used as active layers in photovoltaic cells. Poly(3-alkylthiophene) (P3AT) have been widely used as active materials among them. P3HT (Fig. 11) is the most widely used P3AT material in solar applications and it reported an efficiency of 5% [74, 75].

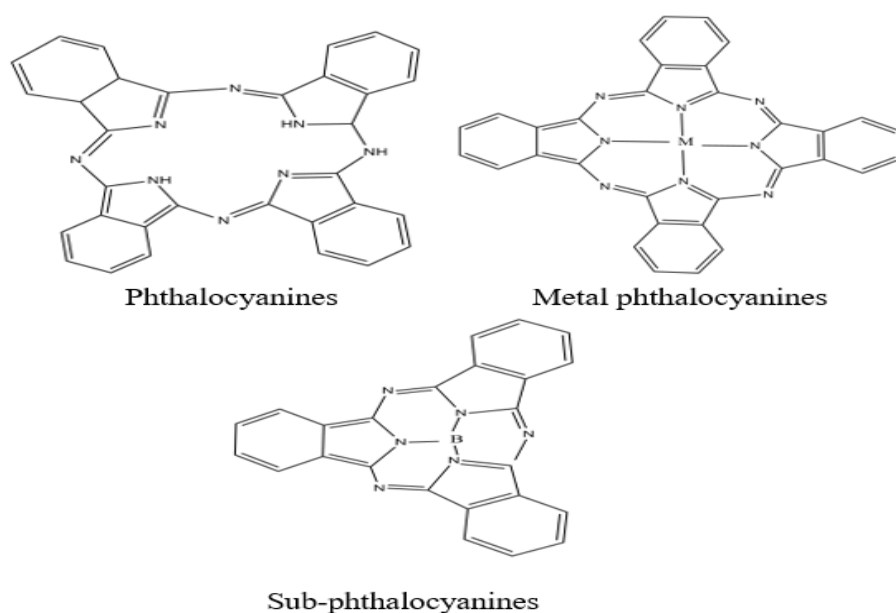


Figure 1.10. Some examples of electron-donor materials

### 1.7.2 Electron-acceptor materials

Organic photovoltaic cells have used a variety of electron-acceptor organic materials over time, including conjugated polymers and tiny molecular compounds. However, only a few of these materials have demonstrated the potential for application in high-efficiency OPV devices.

Fullerenes and their derivatives (Fig.1.12) are well-known and successful electron-acceptor materials, with C<sub>60</sub> exhibiting exceptional symmetry and molecular orbital arrangements that give rise to intriguing chemical and physical properties [76]. In recent years, PC<sub>60</sub>BM and its derivative PC<sub>70</sub>BM have been widely used as acceptors in OPVs due to their advantageous solution process ability. PC<sub>70</sub>BM has superior visible range absorption compared to PC<sub>60</sub>BM, but its extensive purification process makes it more expensive, limiting its widespread application in OPVs [77]. Other than fullerenes, the derivative known as indene fullerene has been used as an electron acceptor material in organic photovoltaics (OPVs).

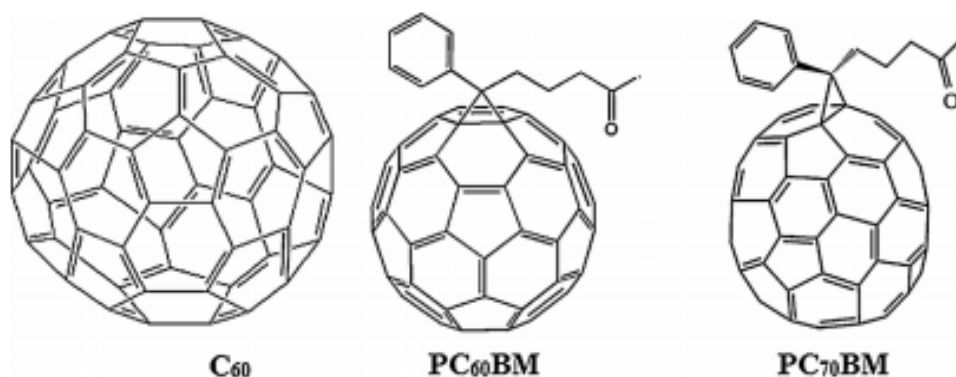


Figure 1.11. some examples of electron-acceptor materials

### 1.7.3 Donor-acceptor polymer

In OPV devices, the donor material has traditionally been responsible for absorbing light because most fullerene acceptors do not strongly absorb in the visible and near-infrared spectrum, where solar radiation is at its peak. Consequently, a significant portion of research has been dedicated to decreasing the optical bandgap ( $E_g$ ) of the polymer. Donor-acceptor (D-A) hybridization, which incorporates alternating electron-rich and electron-poor segments along the polymer backbone, is now widely used. The molecular orbital mixing between the conjugated donor (D) and acceptor (A) units produces hybridized molecular orbitals with a reduced effective bandgap ( $E_g$ ) compared

to each individual component. Due to their ability to create much lower bandgaps than through backbone planarization alone, D-A polymers are becoming more and more common in OPV research [78-80].

#### **1.7.4 Electron donor-acceptor-donor (D-A-D)**

Organic solar cells have the potential to enable the development of economically feasible photovoltaic devices that use environmentally acceptable technology with a low environmental impact. Although soluble conjugated polymers remain an important category of materials utilized as donor in organic photovoltaics (OPV) [81-84]. Over the past years, there's been a rising focus on small molecule donor materials. Their precisely defined chemical structure offers advantages in synthesis reproducibility, material purification, and device performance compared to polydisperse polymers [85]. Using molecules also simplifies the analysis of structure-property relationships, crucial for designing effective photovoltaic materials. In recent years, symmetrical molecules with a donor-acceptor-donor (D-A-D) structure from diverse active molecular material classes have attracted the interest of researchers as donor materials[86-88].

### **1.8 Computational Studies**

Computational chemistry analyzes the behavior and properties of molecules using simulations, algorithms, including ab initio methodologies based on quantum chemistry and empirical methods[89].

Computational chemistry employs a diverse range of algorithms and equations to address chemical challenges. The field of computational chemistry offers a dependable methodology for predicting the diverse properties of molecules that are not feasible to determine experimentally. Furthermore,

it aids in facilitating experimental chemistry to determine the optimal mechanism or methodology. The utilization of theoretical chemistry techniques, integrated with advanced computer programs, is employed to calculate the molecular structures, energies, and characteristics. These methods encompass ab-initio, semi-empirical, Molecular mechanics, molecular dynamics, and Density Functional Theory (DFT) approaches[90].

The computational methods are usually based on classical and quantum mechanics.

### **1.8.1 Classical Mechanical Methods**

Methods that are based on classical mechanics commonly include the molecular mechanical approach and the molecular dynamics method. Both of these methods use Newton's law[91].

#### **1.8.1.1 Molecular Dynamics (MD)**

Molecular dynamics refers to the utilization of computer simulations for the purpose of analyzing the dynamic behavior of molecules and atoms. In the discipline of Molecular Dynamics (MD), the paths followed by atoms and molecules are governed by the numerical solution of Newton's equation of motion. This equation describes the behavior of a system consisting of interacting particles, with the forces between these particles and their associated potential energies often evaluated using interactions between atoms or molecular mechanics-based force fields[92].

#### **1.8.1.2 Molecular Mechanics (MM)**

Molecular mechanics is a branch of classical mechanics that uses the Born-Oppenheimer approximation to create a model of the molecular system. All systems' potential energies are determined by the force field as a function of their nuclear coordinates[93].

## **1.8.2 Quantum Mechanical Methods**

Quantum mechanical (QM) approaches consider the movement of electrons in a molecule to be influenced by the nucleus. Quantum mechanical (QM) procedures primarily entail the solution of the Schrödinger equation, subject to specific approximations, in order to ascertain the electronic configuration, energies, and atomic forces within a molecular system. These technologies also provide chemical pathway details and thermodynamic data like heat of production. Quantum mechanics-based computational methods include *ab initio*, semi-empirical, and DFT [94].

### **1.8.2.1 Ab- initio method**

The *ab initio* approach, which relies on the Schrödinger equation, is employed to determine the energy of a molecule by the utilization of the wave function ( $\psi$ ). The wave function, which is employed to ascertain the spatial distribution of electrons, which in turn allows for the prediction of various molecular properties. The *ab initio* method is characterized by a significantly longer computational time requirement when compared to semi-empirical methods [95].

### **1.8.2.2 Semi-Empirical method**

The semi-empirical approach depends upon the principles of the Schrödinger equation.

The approach involves integrating experimental data with theoretical principles, wherein the experimental results are utilized to parameterize the Schrodinger equation. The semi-empirical method is more time-efficient in comparison to the *ab-initio* method [96].

### **1.8.2.3 Density functional theory (DFT) methods**

Density functional theory (DFT) methods have demonstrated high efficiency in the analysis of molecular characteristics. Density functional theory (DFT) approaches are founded upon the

Schrödinger equation, which describes the energy of a particle. In this context, the energy is dependent on the electron density, which, in turn, is a function of the spatial coordinates (x, y, z).

The application of Density Functional Theory (DFT) encompasses a wide range of electronic properties, including geometry optimization, frontier orbital energies, solvation behavior, potential energy surfaces, Hirschfield charge analyses, and spectroscopic investigations such as infrared (IR) and nuclear magnetic resonance (NMR). The hypothesis proposed by Kohn and Sham examines the electron density and its correlation with the molecular energies in the given equation[97].

$$\mathbf{E} = \mathbf{E}^{\mathbf{V}} + \mathbf{E}^{\mathbf{T}} + \mathbf{E}^{\mathbf{J}} + \mathbf{E}^{\mathbf{XC}}$$

Where:

$E^{\mathbf{V}}$  represents potential energy.

$E^{\mathbf{T}}$  represents the concept of kinetic energy.

$E^{\mathbf{J}}$  accounts for electron-electron repulsion energy.

$E^{\mathbf{XC}}$  represents electron exchange-correlation energy.

Due to various assumptions in the DFT technique, it was further subdivided into two types, including the following:

### 1.8.2.3.1 LDA (Local Density Approximation)

This approximation constitutes a significant category of estimation for the electron correlation energy in Density Functional Theory (DFT), which is predicated on the assessment of electron density at every spatial coordinate. The accuracy of this estimation relies on the assumption of a homogenous electron density within a given molecule. In any scenario, the utilization of the Local

Density Approximation (LDA) estimation method may not be highly appealing for particles exhibiting non-uniform electron density [98].

#### 1.8.2.3.2 Gradient Generalized Approximation

The GGA method can be considered as an extension of the LDA approach, specifically designed to handle non-uniform electron density estimates. The GGA correlation energy approach is considered very suitable for investigating the intermolecular interactions involving two or more molecules [99].

# Chapter 2

## Literature Review

In this chapter, we will explore the significant advancements and critical insights into the utilization of organic materials in photovoltaic cells. The potential of organic photovoltaics (OPVs) to significantly alter the nature of renewable energy production has garnered a lot of interest in recent years. In this article, we will examine the fundamental ideas behind organic materials in solar cells, as well as their most recent advancements, problems, and potential future applications. We'll look into the basics of OPVs, talk about the different organic materials that go into making them, dissect the most recent research, and highlight the positive environmental and economic effects of this innovative technology. Our goal with this review is to provide a thorough analysis of the current status of organic materials in solar cells and to throw light on the prospects for their general use in the production of clean energy.

### **2.1 History of Photovoltaics**

In the year 1839, Becquerel made the significant discovery of the photovoltaic effect. This phenomenon was seen when platinum electrodes, coated with silver halogen, were subjected to illumination in an aqueous solution. It is also referred to as the photo electrochemical effect. [100]. Subsequently, during the period of 1875-1880, William Adams and Richard Day observed a similar outcome in selenium that was positioned between two metallic electrodes, so establishing the initial solid-state photovoltaic device. [101]. This device's photovoltaic effect was dependent on the use of metal and selenium. In 1883 Charles Frits created the first large-area photovoltaic

device, furthering the field's development. These early cells had an electrode made of metal, a semiconductor, and a thin, semitransparent metal electrode with a bottle neck design that allowed incident light to pass through. The constrained design, however, led to a power conversion efficiency of under 1% [102].

PV cells made considerable advancements and obtained useful uses in the 1950s. In 1954, Bell Labs unveiled the first high-power silicon photovoltaic cell with a PCE of 6% [17]. The US Vanguard I satellite initially used a PV array-powered radio in 1958, making it the first commercial application of the technology. However, each had its limitations. Other PV cell materials like cadmium sulphide, gallium arsenide, cadmium telluride, and indium phosphide were also investigated. Due to their advantages, silicon-based PV cells were regarded as the most promising technology [18]

During the 1970s, the global oil crises spurred increased research and development in photovoltaic (PV) technology, leading to significant improvements in PV cell performance. The research was centered on the advancement of device physics and process technologies [103]. Methods for lowering the manufacturing costs of thin film technologies based on amorphous or microcrystalline silicon were also extensively researched. During this time, researchers studied tandem cell architectures and band gap tuning of semiconductor materials in order to enhance power conversion efficiency [104]. However, mass manufacturing of infrared for semi-conducting devices was not yet sufficiently progressed, and production prices were still exorbitant in comparison to those of oil.

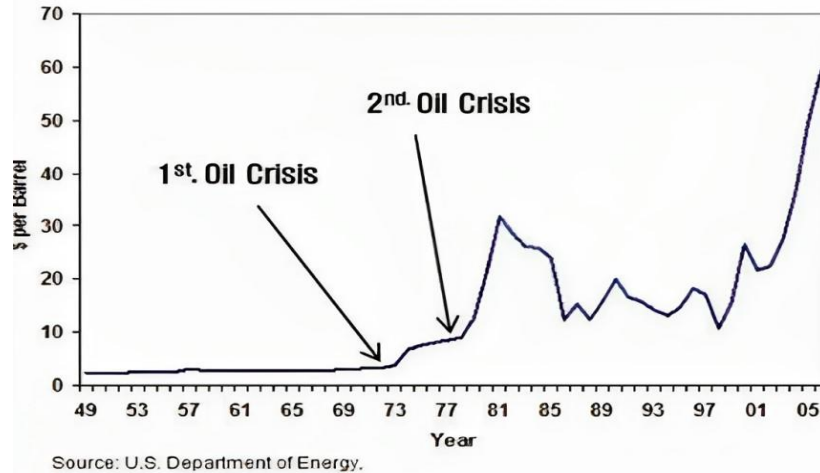


Figure 2.1. Overview of the oil price

During the 1990s and 2000s, there was a huge increase in interest in photovoltaics. This increased focus can be linked to a variety of factors, including energy deregulation and growing worries about environmental problems such as climate change. These concerns have contributed to a strong drive to investigate and secure alternate energy sources [105]. Notably, the rise in oil costs, with the cost of one barrel reaching around \$150.00, has prompted governments and businesses to actively investigate other energy sources in order to reduce their reliance on oil. Additionally, governments in many countries provide discounts for 1/3 to 1/2 of the total installation costs of PV systems, which has sped up the development of significant PV technology-based businesses. PV technology started to have an impact on the world in the initial ten years of the 20th century by promoting the shift from fossil fuels to renewable sources of energy [18].

Photovoltaics are gaining popularity as a viable alternative to fossil fuels because of their low upfront costs, high efficiency, and unlimited potential for future use[106]. Currently, materials utilized in photovoltaic cell including monocrystalline silicon, polycrystalline silicon, amorphous silicon, cadmium telluride, copper indium gallium, and copper indium gallium selenide. The efficiency of photovoltaic systems has experienced substantial advancements in recent years[107].

Silicon cells have an impressively high rate of efficiency, but their application is restricted due to the rigidity of their structures and the lengthy period of time required for the repayment of cost and electricity. New solar technologies like OPVs may fill gaps in inorganic PV. Scalable roll-to-roll manufacturing on flexible substrates makes them advantageous. The cost is lower and the applications are wider.

## **2.2 Organic Photovoltaic cells**

Organic photovoltaic cells are a highly advantageous cost-effective and environmentally friendly alternative to silicon-based solar cells due to their reduced molecular weight, solution-processing capabilities, flexibility, compatibility with flexible substrates, potential for large-scale manufacturing, and cost-effective fabrication methods, attracting significant scientific interest[108].

## **2.3 Organic Materials in PV cells**

The design of materials that are active on the basis of well-defined molecules is gaining attention for developing cost-effective and environmentally friendly organic photovoltaic cells (OPV). In contrast to polydisperse conjugated polymers, properly defined molecular donors improve synthesis and purifying consistency. More control over material composition and device performance results. More importantly, molecules enable more accurate analysis of structure-properties connections, advancing material design[109].

### **2.3.1 Donor Materials**

In recent years, many kinds of molecular donors have been synthesized and assessed as potential donor materials in both vacuum-deposited and solution-processed and organic photovoltaic (OPV) cells.

### **2.3.1.1 Phthalocyanines**

Phthalocyanines are most frequently used as the donor units in these photoactive molecules because of their excellent light-harvesting abilities. Organic thin-film solar cells with a bulk heterojunction design, using phthalocyanines derivative C6PcH<sub>2</sub>, have shown outstanding performance metrics. The cells have an indium–tin-oxide/polymer hole transport layer/C6PcH<sub>2</sub>:PCBM/Al structure, with an energy conversion efficiency of 3.1% and an external quantum efficiency of over 70% within the Q-band absorption area[110].

### **2.3.1.2 Tin (II) phthalocyanines**

The study examined the performance of organic solar cells (OSC) using tin (II) phthalocyanines (SnPc)/C<sub>60</sub> heterojunction, analyzing the effect of SnPc thickness on device electrical properties. The results showed 0.79% power conversion efficiency at 1.5G solar illumination[111].

### **2.3.1.3 Metal phthalocyanines**

Metal phthalocyanines (m-Pc) donors excel in organic solar cells (OSCs) compared to traditional ones (CuPc, ZnPc). Varying donor-to-acceptor ratios for different m-Pc donors enhances performance in Schottky OSCs with high acceptor content. Chloroindium phthalocyanines (ClInPc):C<sub>60</sub> OSCs offer near-IR absorption potential, suggesting high efficiencies and voltages above 1 V. The study shows that the J<sub>sc</sub> depends on balancing m-Pc Q band and C<sub>60</sub> aggregate absorption, making ClInPc a suitable donor for semi-transparent OSCs. The easy synthesis and purification of m-Pcs could lead to cheap and efficient organic photovoltaics[112].

#### **2.3.1.4 Copper phthalocyanines**

Copper phthalocyanines (CuPc) purity affects small-molecular-weight organic double hetero junction's donor-acceptor bilayer solar cells. Enhanced CuPc purity increases power conversion efficiency from  $0.26 \pm 0.01\%$  to  $1.4 \pm 0.1\%$  under AM1.5G, 1 sun illumination. Unpurified CuPc has roughly three order of magnitude poorer hole mobility than pure material. Metal-free phthalocyanines is the major contaminant, reducing device performance and hole mobility[113]. Copper phthalocyanines nanoparticles (CuPc-NPs) as a buffer layer in organic solar cells (OSCs), enhancing photovoltaic parameters. The optimized OSC showed a power conversion efficiency of 5.22%, a fill factor of 0.465, and Voc 0.24 to 2.57 (average 1.29), attributed to improved interface characteristics and efficient charge transfer[114].

#### **2.3.1.5 Sub- phthalocyanines**

SubPc is commonly utilized as an electron-donor material in OPV due to its superior energy-level alignment. Beaumont et al. recently discovered that Tc: SubPc OPV devices with tetracene (TC) as an electron donor and SubPc as an electron acceptor achieved 2.9% efficiency[115].

Interfacial engineering improves organic solar cell (OSC) performance by optimizing charge transfer, collection, and recombination. Conventional PTB7-Th: PC71BM OSCs use non-conjugated tetrasodium iminodisuccinate (IDS) as an electron transport layer, boosting power conversion efficiency to 9.45%[116].

#### **2.3.2 Acceptor Materials**

In order to function properly, BHJ devices need an electron acceptor in addition to the light-absorbing polymer donor. Since the beginning of OPV research, the materials that have been employed for this purpose have nearly always been a fullerene and fullerene derivatives. One

example of this type of material is the prototypical phenyl-C61-butyric acid-methyl ester (PC61BM)[77].

### **2.3.2.1 Fullerene (C60)**

An organic solar cell using fullerene (C60) as the acceptor requires a thin buffer layer to achieve a high power conversion efficiency. The scientists suggest that the buffer layer in organic solar cells prevents electron transmission from metal to C60, promoting free carrier collection with a desirable electric field. The transient photovoltaic method confirmed this hypothesis, suggesting the buffer layer is not responsible for the excitons blocking effect[117].

Mixed films of boron sub phthalocyanines chloride (SubPc) and C60 are examined for organic photovoltaic cells. These cells perform best at 80% C60, but the SubPc-to-C60 ratio greatly affects efficiency. The active layer's structural pattern improves with this blend, increasing hole mobility. The improved SubPc:C60 ratio produces organic photovoltaic cells with a  $3.7 \pm 0.1\%$  power conversion efficiency under simulated solar light[118].

The use of solution-processed blends in photovoltaic cell development, focusing on anthradithiophene derivatives as donor materials and fullerene derivatives as acceptors. Solvent vapor annealing creates spherulites, which directly impact performance. A high-performing cell with 82% spherulites coverage achieved a 1% power conversion efficiency, demonstrating the potential of solution-processed small molecule photovoltaic cells.

### **2.3.2.2 Fullerene derivatives**

Polymer solar cells (PSCs) are made up of conjugated polymers and soluble fullerene acceptors, used between electrodes for light conversion. PC60BM and PC70BM are widely used, but recent advancements in fullerene derivatives have led to the development of other materials with

improved characteristics. This paper analyzes recent synthesis and characterization of these derivatives, focusing on their potential to enhance the efficiency of photovoltaic solar cells[119].

#### **PC60BM and PC70BM**

Different electron acceptors (PC60BM or PC70BM) of P3HT-based polymer solar cells (PSCs) were examined. Strong visible absorption in PC70BM-based cells increased efficiency (Voc: 0.62 V, Jsc: 11.85 mA/cm<sup>2</sup>, PCE: 3.52%). PC60BM cells had decreased absorption and measures (Voc: 0.58 V, Jsc: 10.68 mA/cm<sup>2</sup>, PCE: 3.02%). Due to molecular size, PC70BM increased photon absorption and charge transport. Photon absorption, exciton dissociation, and transport of charges affect performance[120].

#### **Indene-C70 Bisadduct**

The widely used acceptor material PC60BM has limitations in polymer solar cells due to low energy levels and poor light absorption. To address this, a new soluble C70 derivative called indene-C70 Bisadduct (IC70BA) is developed with a higher LUMO energy level. IC70BA outperforms P3HT-based PSCs, providing higher voltage and better power conversion efficiency, making it a potential replacement for efficient PSCs[121].

Polymer solar cells with P3HT as a donor and IC70BA as an acceptor show improved photovoltaic performance when 3 vol% of MT or HT as processing additives are added. UV-vis absorption spectroscopy, X-ray diffraction, and atomic force microscopy show increased absorbance, crystalline structure, and film shape. Power conversion efficiency (PCE) increases from 5.80% without additives to 6.69%[122].

### **2.3.3 Donor-Acceptor materials**

Since fullerene acceptors are weak in the visible and near-IR spectrum, when solar radiation is most intense, the absorption of light in OPV devices typically falls on the donor. This implies that

many Studies have reduced the optical band gap  $E_g$  of polymer. Semiconducting polymers' bandgap is caused by  $\pi$ -orbital overlap, which can be reduced by creating a polymer backbone with enhanced planarity, thereby extending conjugation. Chemists have used various methods, such as fused ring systems (e.g., benzodithiophene and thienothiophene) and bridging atoms (e.g., fluorene, cyclopentadithiophene), to reduce the optical bandgap of the polymer. They have also increased the quinoidal character and minimized torsion along the polymer backbone. A (Donor-Acceptor) polymers including the benzo[1,2-b:4,5-b] dithiophene (BDT) unit have gained amazing success in the last decade, with single junction and tandem devices currently reaching 10% efficiencies [123-125].

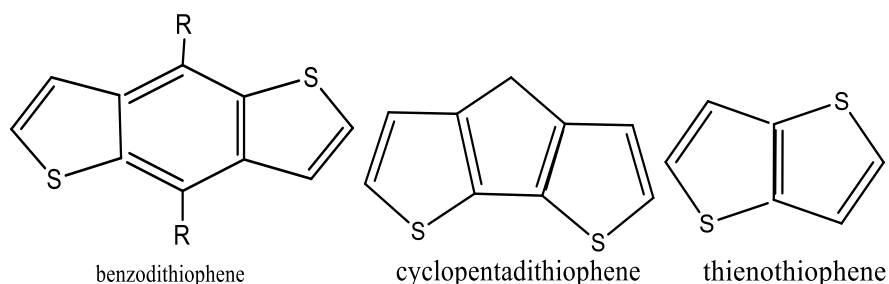


Figure 2.2. Some examples donor-acceptor polymers

### 2.3.3.1 Benzodithiophene (BDT)

The electron-rich benzodithiophene (BDT) unit is ideal for conjugated polymers. The symmetrical and coplanar structure of the material allows for efficient charge movement through intermolecular  $\pi$ - $\pi$  interactions. Benzodithiophene (BDT) polymers were developed and produced for organic field-effect transistors. These polymers exhibit a remarkable hole mobility value of  $0.25 \text{ cm}^2/\text{Vs}$ [126]. Yang and colleagues in 2008 introduced BDT-based donor-acceptor conjugated polymers for organic photovoltaics (OPVs)[127]. The thieno[3,4-b]-thiophene (TT) unit is a unique thiophene-based building block used in synthesis of p-type conjugated polymers due to its ability to adapt a quinoidal resonance structure along the conjugated backbone, resulting in lower energy of bandgap.[84, 128, 129]

A new photoactive donor for organic solar cells (OSCs) is a benzodithiophene-based donor-acceptor-conjugated polymer (P1). P1 dissolves in halogenated and non-halogenated organic solvents and has a broad absorption curve. The PCE of chlorobenzene polymer was 2.79%, but diphenyl ether raised it to 5.33%. This shows the polymer could improve efficiency, producing a new class of high-performance, air stable OSC polymers[130]. Four new donor-acceptor copolymers were synthesized using benzo[1,2-b:4,5-b'] dithiophene and benzo[1,2-b:4,5-b'] difuran as donor components and thieno[3,4-b] thiophene as acceptor. Poly[(4,8-bis(5-dodecyl-2-furanyl) benzo[1,2-b:4,5-b'] difuran-2-yl)-alt-(2-ethyl-1-(3-fluorothieno[3,4-b] thiophen-2-yl)-1-hexanone)] was used in bulk heterojunction solar cells, with P4 achieving the best power conversion efficiency is 5.23% [131].

#### **2.3.3.4 Coplanar tricyclic dithiophene (CPDT)**

Coplanar tricyclic dithiophene materials for generating organic molecules suitable for various optoelectronic applications. By altering the bridging atoms, the structural molecular characteristics of these formations can be modified. Carbon-bridged 4H-cyclopenta[2,1-b:3,4-b']dithiophene (CPDT) was initially crucial for the production of donor-acceptor conjugated polymers, particularly for polymer solar cells (PSCs)[132-134].

The CPDT bridging carbon can be functionalized with two alkyl groups to improve copolymer solubility. Zhu and colleagues developed poly[2,6-(4,4-bis(2-ethylhexyl)-4H-cyclopenta[2,1-b:3,4-b'] dithiophene)-alt-4,7-(2,1,3-benzothiadiazole)] (**P1**), a solid-state thin film with strong interchain interactions and a 760 nm absorption peak. **P1** achieved a 3.5% power conversion efficiency when combined with PC71BM in 2007[135].

Scherf et al, presented a CPDT-based D-A alternating copolymer **P2** with 4,7-di(thiophen-2-yl) benzo[c][1,2,5] thiadiazole as a comonomer. The **P2**: PC61BM (1: 1) blend, employing a solvent mixture of chlorobenzene and anisole (19: 1, v/v), achieved a PCE of 2.1% [136].

### **2.3.3.3 Naphthodithiophene (NDT3)**

A new class of semiconducting polymers, derived from Naphthodithiophene (NDT3), has been studied for their large system and donor-acceptor structure, contributing to their tight stacking. PNNT3NTz-DT is a flexible polymer with a 5% power conversion efficiency and high field-effect mobility, making it a promising core unit for semi-conducting polymers and a promising design method for high-performance polymers [137].

### **2.3.4 Donor-Acceptor-Donor**

Organic photovoltaic cells enable cost-effective photovoltaic devices with minimal environmental impact. Soluble conjugated polymers are still the primary donor materials for OPV, however small molecule-based materials are gaining popularity in recent years. The distinct chemical structure of molecules offers advantages over polydisperse conjugated polymers in terms of reproducibility, purity, and device performance. However, molecules enable easier and more accurate investigation of structure-properties connections, making them essential for designing photovoltaic conversion materials[138]. In recent years, conjugated systems generated from symmetrical molecules having a D-A-D structure have garnered attention as donor materials among active molecular materials.

Triphenylamine (TPA) has strong electron-donating capabilities and great capacity to assist hole transport, making it a very intriguing choice for organic photovoltaic applications [95]. There has been much research conducted on TPA-based small molecules for use in organic solar cells (OSCs). These small molecules include linear structures with TPA as the terminal group, as well as star-like molecules with TPA as the center [96-98]. A variety of TPA-based small compounds for high-efficiency OSCs have been disclosed by Li and Zhang et al [99].

A TPA-based linear D-A-D small molecule containing a thiazolothiazole (TT) acceptor unit has recently been described, with PCE values as high as 3.73% [100]. A new organic molecule (M1) with a triphenylamine electron donor and isoindigo electron acceptor was created through Stille coupling. M1 absorbs light from 300 to 700 nm, has a low HOMO energy level, and moderate hole mobility. Solar cells achieved 0.84% efficiency[139]

Two new molecules, TPA-TV-PM and TPA-HTV-PM, have been developed for solution-based organic solar cells. These molecules, combining triphenylamine, pyran, and thienylenevinylene, offer wide visible light absorption and lower HOMO energy levels, resulting in solar cell efficiencies of 2.06% and 2.10% under AM1.5 illuminations[140].

Two D-A-D systems with benzo furan and dithienopyrrole as donors and isoindigo as acceptor were synthesized, and their electronic properties were analyzed using UV-Vis absorption and cyclic voltammetry. The presence or absence of nitrogen substitution significantly impacted the material's characteristics and solar cell performance[141].

A symmetrical donor-acceptor-donor (D-A-D) was created by connecting dithienopyrrole donors to a central electron acceptor from dimerized 3-alkoxy-4-cyanothiophene. This compound shows efficient photoluminescence, broad absorption, and a 1.70 eV band gap. In bulk heterojunction solar cell tests, it achieved a conversion efficiency of 0.90%[85].

The efficiency of D-A-D organic photovoltaic system is crucial for their practical application as low cost and renewable energy sources. While previous studies have examined factors such as donor acceptor selection, molecular structure design and interface engineering, the specific influence of carbon chain length on the efficiency of D-A-D OPV systems warrants further investigation. Increasing the carbon chain length has been proposed as potential approach to

enhance absorption and charge transport properties, but a systematic evaluation of this factor's effectiveness compared to others is currently lacking.

Table 2.1. Summary of organic materials, and their efficiency ranges reported in the literature.

Sr. No.	Author/s	Materials Studied	Efficiency	Year
1	Hori, T., et al.	Phthalocyanines (C6PcH2)	3.1%	2010
2	Du, C., et al.	Tin (II) phthalocyanines (SnPc)/C60	0.79%	2011
3	Beaumont et al.	Tc: SubPc	2.9%	2012
4	Zhang, F., et al	(PC60BM or PC70BM) of P3HT based PSCs	3.52%	2014
5	Huang, P., et al	Benzodithiophene-based polymers	5.23%	2015
6	Scherf et al.	CPDT-based D-A alternating copolymer	2.1%	2014
7	Osaka, I., et al.,	Naphthodithiophene-based polymers	5%	2012
8	Chen, M., et al.	TPA-TT small molecule	3.73%	2017
9	Yang, M., et al.	M1 (Triphenylamine and isoindigo)	0.84%	2013
10	Zhang, J., et al.	TPA-TV-PM and TPA-HTV-PM	2.06% / 2.10%	2015
11	Yassin, A., et al.	Benzo furan and dithienopyrrole	2.10%	2013
12	Yassin, A., et al.	Dithienopyrrole and 3-alkoxy-4-cyanothiophene	0.90%	2012

### **Aims and Objectives**

To the best of our knowledge, the major focus of research on organic photovoltaic cell is on the donor and acceptor units, however, the carbon chain linking the donor and acceptor unit needs to be investigated. This research aims to improve organic photovoltaic (OPV) cells by studying the carbon chain length between the donor-acceptor and acceptor-donor units of D-A-D organic materials. The primary objective is to determine the most favorable carbon chain length that improves the efficiency and stability of organic photovoltaic (OPV) devices. The aims encompass the synthesis and characterization of these materials, investigation of their optical and electrical properties, and evaluation of their influence on the performance of organic photovoltaic devices.

# Chapter 3

## Methodology

The central objective of this research was to apply DFT calculation to evaluate the effective length of Carbon chain between Donor-Acceptor and Acceptor-Donor parts of D-A-D structures. The methodology consisted of three distinct steps, as described below:

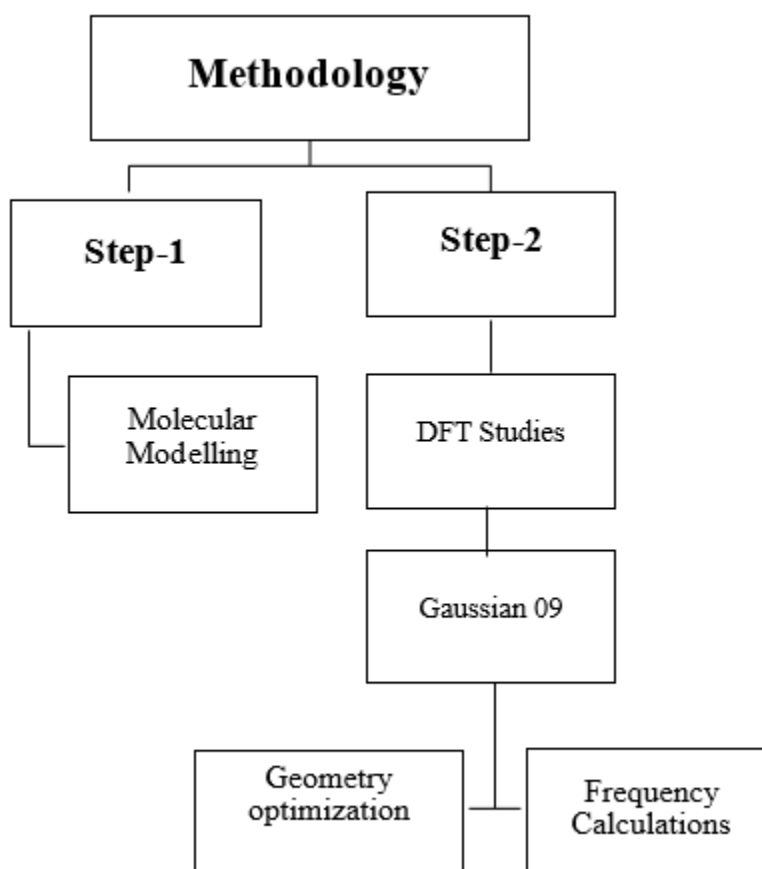


Figure 3.1. Methodology Flow chart of Computational Modelling

### **3.1 Molecular Modelling**

Molecular modeling is the scientific approach used to represent the structural arrangement of molecules in three-dimensional space, utilizing x, y, and z coordinates. These structures are then subjected to geometry optimization, ensuring compliance with fundamental chemical laws and theories. The field of molecular modeling is vast and holds immense potential. In the past decade, it has evolved to encompass tasks such as optimization, prediction, simulation, and analysis of molecule behaviors in real and passive time. This technique has revolutionized computational science, enabling effective solutions to chemical problems and establishing a new discipline for advancement[142].

Molecular modeling holds a vital position in the advancement and fine-tuning of organic photovoltaics (OPV)[143], a research field dedicated to designing and producing efficient solar cells utilizing organic materials. By employing computational techniques, scientists can explore and enhance the performance of OPV systems.

In the present study, the application of molecular modelling was employed to construct an organic molecule. Specifically, the investigation focused on the impact of increasing the carbon chain length between the Donor-Acceptor and Acceptor-Donor moieties in D-A-D structures. This research endeavor aimed to enhance comprehension and facilitate further advancements in this particular field of study. The GUI Gauss-View06 program was used to model all of the molecular geometries.

#### **3.1.1 GaussView06**

GaussView06 is a widely utilized graphical user interface that is commonly employed alongside the Gaussian computational chemistry software. Its primary purpose is to simplify the setup of

various Gaussian calculations by providing a user-friendly interface. It offers advanced features such as a molecule builder, which allows for the creation of three-dimensional chemical models of molecular systems[144]. Moreover, Gauss View 06 enables users to effortlessly generate and execute Gaussian input files without the need for manual command line instructions. Additionally, it offers exceptional visualization capabilities, allowing for the graphical interpretation of Gaussian output files through features like plots, spectra, and animated vibrations. Overall, GaussView06 streamlines the process of working with Gaussian[145], making it more accessible and efficient for researchers in the field of computational chemistry.

### **3.1.2 Gaussian-09**

Gaussian-09 is a widely utilized software package in computational chemistry, initially developed in 1970 as Gaussian-70 by John Pople and his team[146]. It serves as a valuable tool for chemists, chemical engineers, biochemists, and material scientists to perform diverse computational tasks in chemistry and biochemistry. The software encompasses molecular mechanics (MM), ab initio, Semi Empirical, and Density Functional Theory (DFT) methods, enabling users to calculate molecular structures, properties, and reactions using different levels of theory. A key advantage of Gaussian-09 is its inclusion of built-in standard basis sets, such as STO-3G, 3-21G, 6-21G, 4-31G, 6-31G, LANL2DZ, SDD, and others. These basis sets facilitate efficient and accurate quantum chemical calculations by mathematically describing molecular orbitals. Gaussian-09 stands as a powerful and versatile computational chemistry software package, offering a wide range of methods and basis sets to support diverse computational analyses in the field of chemistry[147, 148].

### **3.2 Density functional theory (DFT)**

Density functional theory (DFT) is a widely used computational approach in computational chemistry that allows for the study of the electronic structure and properties of atoms, molecules, and solids. It is based on the concept of electron density, which describes how electrons are distributed in a given system.

DFT calculations enable researchers to compute and analyze various characteristics of the system, including its energy, structure, and properties. By employing DFT, valuable insights can be gained into the fundamental properties of materials, such as their geometries, electronic energies, ionization potentials, electron affinities, and vibrational frequencies.

Additionally, DFT can be applied to predict and understand chemical reactions, interactions between molecules, and the behavior of materials under different conditions. The computational efficiency of DFT makes it particularly advantageous for investigating complex systems and phenomena, as it strikes a balance between accuracy and computational cost.

In this research, the Gaussian 09 software[149]was utilized for the DFT studies. The output geometries were visualized using the Molden program[150]. Gaussian is a versatile computational chemistry software package that is widely employed for Molecular Mechanics, Semi-Empirical methods, and Density Functional Theory investigations. Specifically, Gaussian-09 was utilized in this study to conduct all the simulations. The DFT calculations involved two main steps:

- Geometry Optimization
- Frequency Calculation

### **3.2.1 Geometry Optimization**

Geometry optimization involves the optimization of a system's geometry, the goal of geometry optimization is to reduce the energy of the molecule by modifying the geometry of a system, particularly the nuclear coordinate of atoms. All modelled geometries are subjected to this optimization method, which makes use of the hybrid density functional B3LYP and LANL2DZ energy levels of DFT[151].

#### **3.2.1.1 B3LYP functional**

The B3LYP functional[152], which stands for Becke's three-parameter exchange with Lee, Yang, and Parr correlation functional, is well known and frequently used in quantum chemistry. It is the most well-known and widely used hybrid functional model due to its extraordinary capacity to properly predict molecule structures and several other features[153].

#### **3.2.1.2 6-31G (d) Basis set**

A common basis set in the field of quantum chemistry is the 6-31G (d) basis set[154], which consists of 6 cores and 31 valence electrons. basic functions plus diffuse functions. The 31 basic functions explain the behavior of valence electrons involved in chemical bonding, while the 6 basis function effectively clarify the behavior of core electrons. When dealing with systems with extended electron densities, diffuse functions are added to the basic functions of Gaussian-type functions to improve accuracy. In conclusion, when characterizing the electronic makeup of atoms and molecules, the 6-31G (d) basis set strikes an ideal compromise between computing efficiency and precision.

### 3.2.2 Frequency calculations

Frequency calculations, which examined the molecular system's nuclear vibrational motion in terms of its modes using the same basis set as the geometry optimization, were used to validate the optimized geometries. The optimized geometries' validity is supported by the fact that the frequency calculations don't provide any fictitious frequencies and that they actually match to real energy minima.

### 3.2.3 Molden

Molden is an application of software program used in the field of computational chemistry for the visualization and analysis of molecule electronic structures.

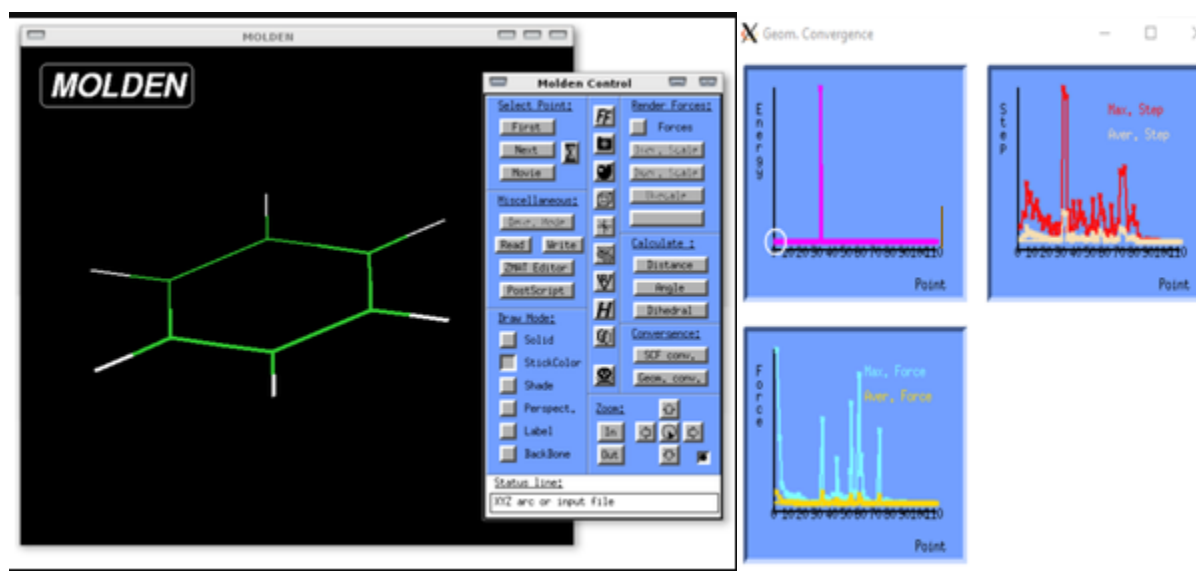


Figure 3.2 Molden: a graphical visualization tool

It displays graphical representations of molecular structures and reads file outputs from quantum chemistry programmed, enabling researchers to understand, and analyzing computational chemistry results.

# Chapter 4

## Results

In this study, we investigated the "Design and Analysis of Donor-Acceptor-Donor Parts of Organic Materials for Photovoltaic Cells" with a focus on the strategic modulation of carbon chain lengths between the donor and acceptor, as well as the acceptor and second donor cells using hybrid functional DFT method B3LYP and exchange-correlation functional basis set 6-31G (d) using Gaussian-09 software. The optimization of organic materials for photovoltaic applications demands a nuanced understanding of their structural and electronic properties. Through systematic design variations, we synthesized a series of donor-acceptor-donor compounds, each distinguished by an increased number of carbon chains between the donor and acceptor components.

### 4.1 Molecular Modeling

The pristine structure (Fig 4.1) was modeled in gauss view. This is the D-A-D (Donor-Acceptor-Donor) structure or, for the understanding purpose we can designate as  $D_1$ -A- $D_2$  structure, type design strategy has been done to improve the charge mobility for the bulk heterojunction concept in pursuit of higher efficiency. In this D-A-D structure two different donor units are attached; triphenylamine (TPA) has been found substituent as a donor-1 to be more beneficial as materials for increasing photovoltaic performance and exhibited wide applications in organic photovoltaics (OPVs) while the second donor is 2,5-dimethylthiophene with the molecular formula  $C_6H_8S$ . In

this molecule central acceptor unit 4,7-dimethyl-[1,2,5]oxadiazolo[3,4-c]pyridine is a heterocyclic compound featuring a fused ring system, combining a pyridine ring with an [1,2,5]oxadiazole ring.

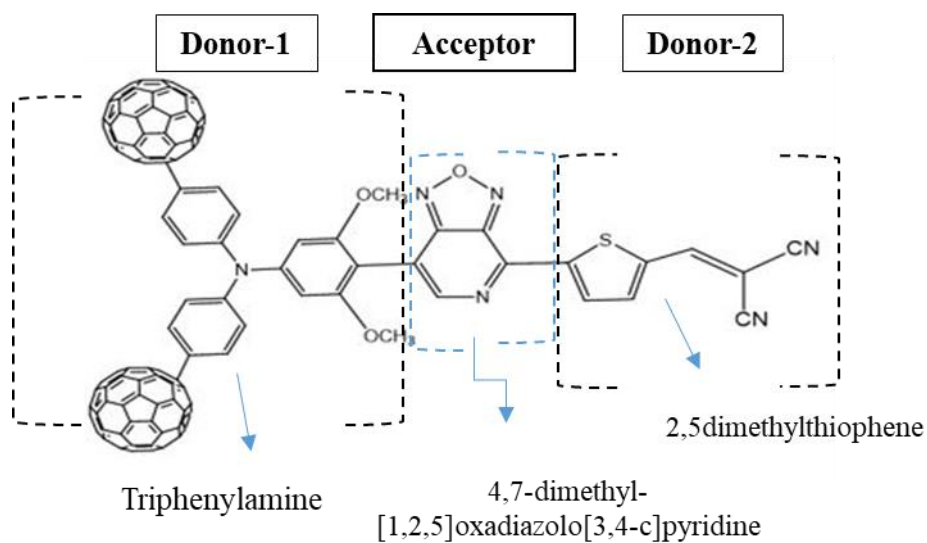


Figure 4.1. Structure of Pristine molecule

In this study, we investigate the systematic variance of the length of the carbon chain between the donor moiety and acceptor, as well as the acceptor and donor moieties within D-A-D structures. Figure 4.2 list donor-acceptor and acceptor-donor carbon atom counts. The data shows a continuous rise in carbon atoms from donor-acceptor to acceptor-donor, revealing structural changes.

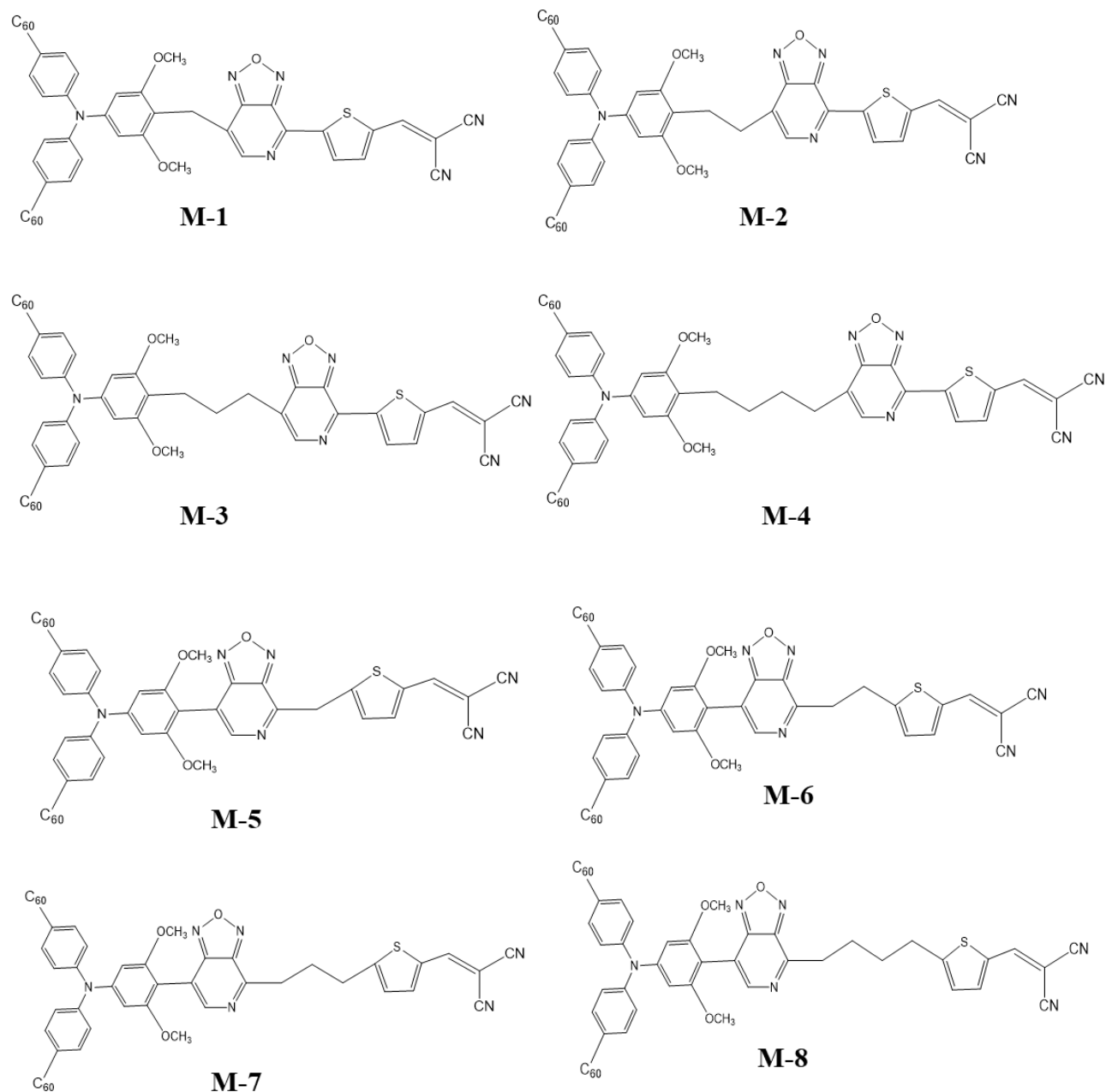


Figure 4.2. 2D structures of molecules, M1-M4 - Number of carbon increase between Donor-acceptor, M5-M8 - Number of carbon increase between Acceptor-donor

## 4.2 Geometry optimization

The optimized geometry obtained served as a visual representation of the conformation of the molecule that was most stable, characterized by the lowest potential energy. It is an indication of

the stability of the molecule conformation that this number represents the minimal energy state that was attained during the iterative optimization process.

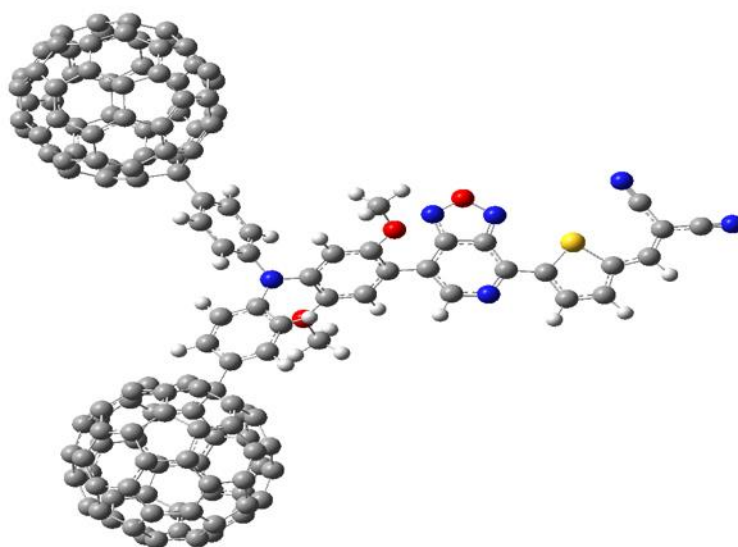


Figure 4.3. Optimized Structure of Pristine molecule

In the pursuit of enhancing the pristine molecular structure, a systematic optimization approach was employed to investigate the impact of increasing the number of carbon atoms between the donor and acceptor moieties. To achieve this, successive modifications were made by incrementally inserting carbon atoms one by one between the donor and acceptor groups. The optimization process, carried out through computational methods, aimed to refine the molecular architecture and evaluate the resulting energy landscape.

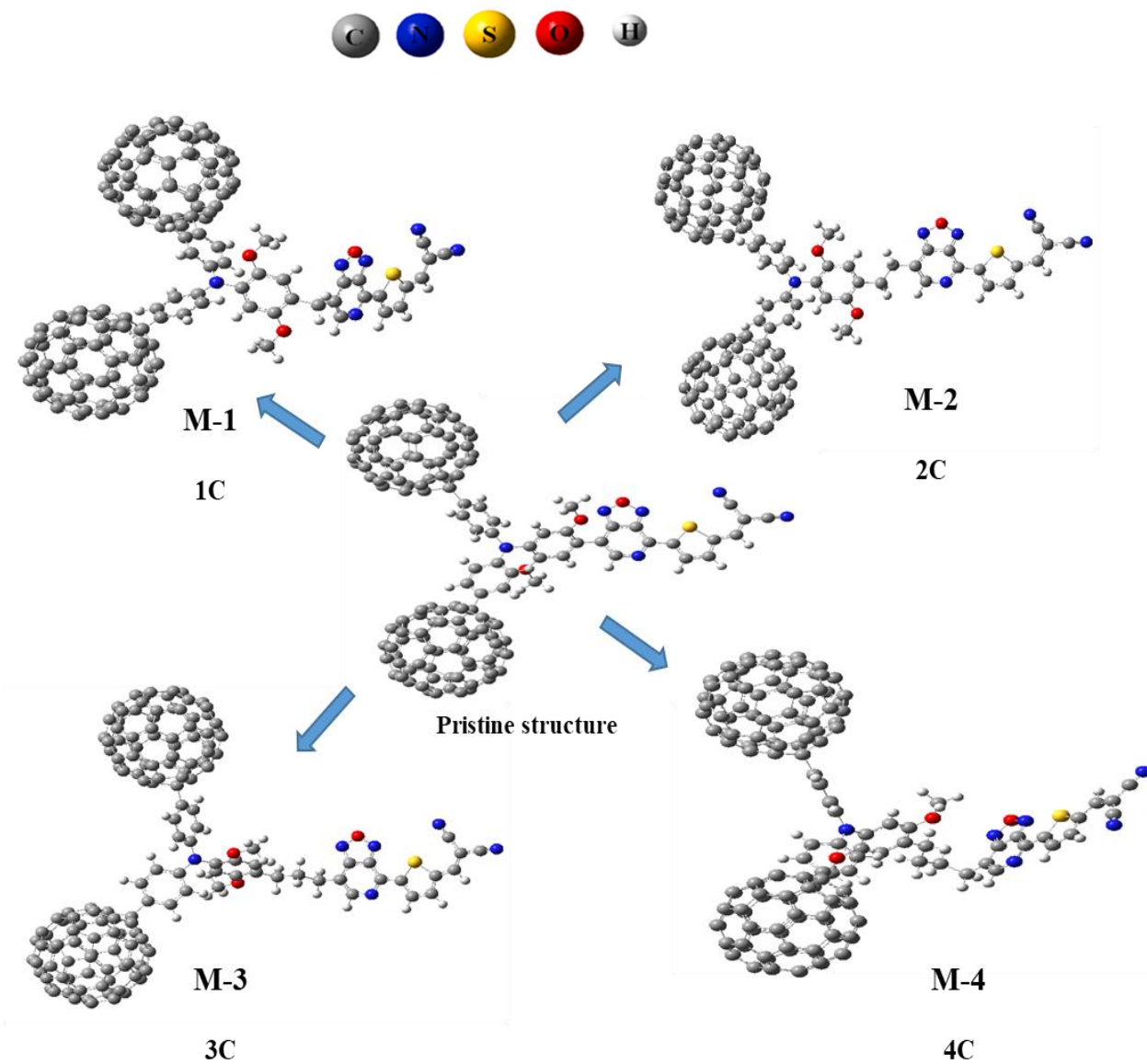


Figure 4.4. Optimized geometries of M1-M4 using B3LYP/6-31G(d) level of DFT.

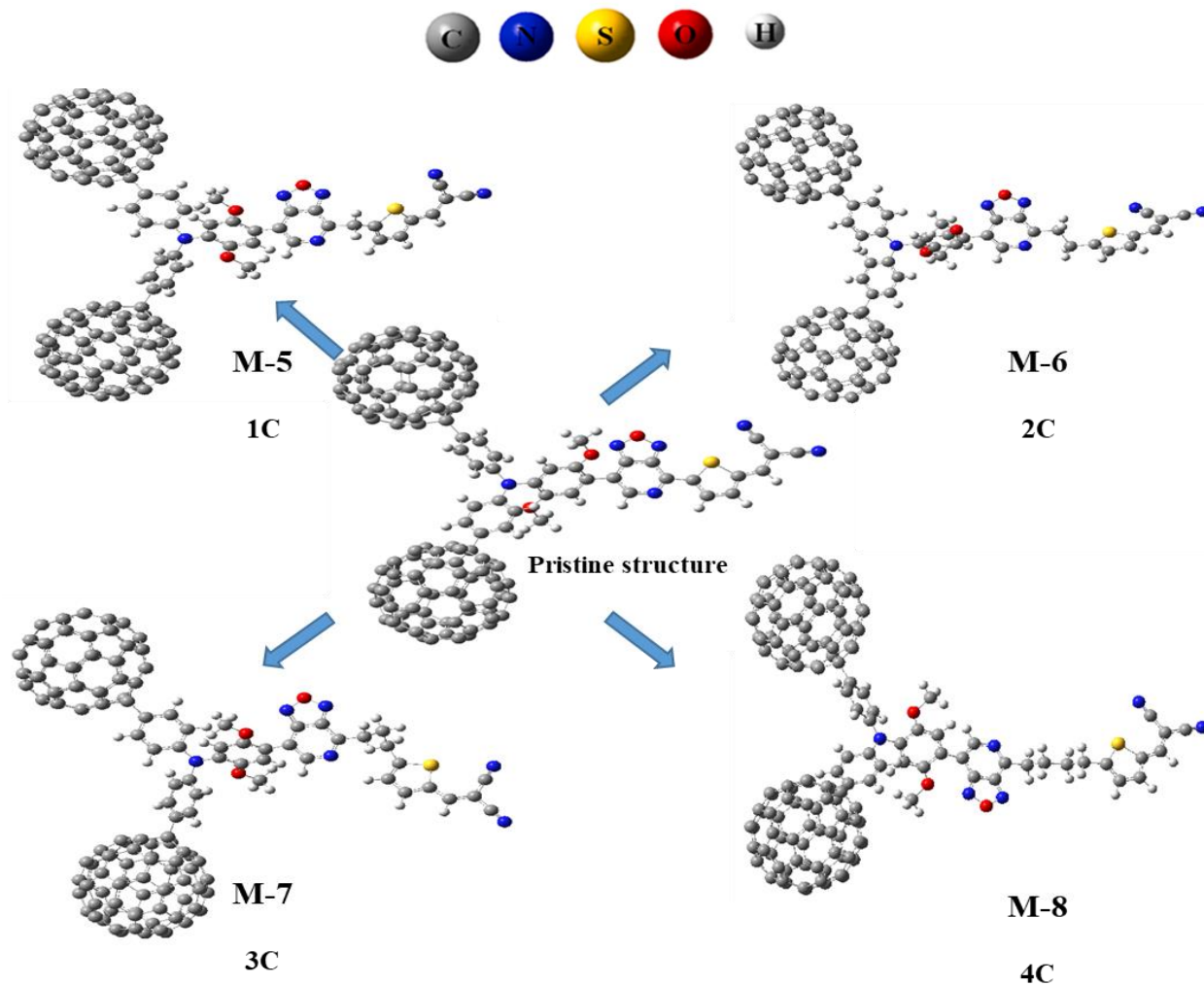


Figure 4.5. Optimized geometries of M5-M8 using B3LYP/6-31G(d) level of DFT

Table 4.1. The Energy value of Optimized geometries of M1-M8 in eV

S No.	Structures	Optimization Energy	Relative energy
1	Pristine	-6794.028	0.0
2	Mol-1	-6833.343	32.8
3	Mol-2	-6872.653	32.8
4	Mol-3	-6911.970	32.7
5	Mol-4	-6951.279	32.9
6	Mol-5	-6833.337	32.9
7	Mol-6	-6872.654	32.8
8	Mol-7	-6911.971	32.7
9	Mol-8	-6951.284	32.7

According to optimized data (Table 4.1) for the model geometries Mol-1 to Mol-8, the relative energy increases to ~32.8 eV with the addition of each methyl group between the Donor-1 and Acceptor part or Acceptor and Donor-2 part of pristine molecule.

### 4.3 HOMO-LUMO Energy Gap

The highest occupied molecular orbital (HOMO) and the lowest unoccupied molecular orbital (LUMO) play a crucial role in understanding the electronic structure and reactivity of molecules. Because they may be used to forecast how a molecule would interact with other species, the frontier orbitals got their name. Since HOMO is regarded to be the orbital with the most electrons, it frequently serves as an electron donor for those electrons. On the other hand, LUMO is the innermost orbital that has open spaces for electrons to enter. As a result, although the energy of the HOMO is inversely proportional to the ionization potential, that of the LOMO is inversely correlated with the electron. The energy gap, which describes the stability and reactivity of the structure, is the difference in energy between the HOMO and LUMO orbitals.

Table 4.2.HOMO-LUMO energy values and Energy gap values of Pristine and M1-M8

Structure	HOMO (eV)	LUMO (eV)	Energy gap (eV)
Pristine	-4.619	-4.404	0.216
Mol-1	-4.544	-4.319	0.224
Mol-2	-4.558	-4.357	0.201
Mol-3	-4.507	-4.27	0.237
Mol-4	-4.532	-4.319	0.213
Mol-5	-4.606	-4.404	0.216
Mol-6	-4.59	-4.392	0.214
Mol-7	-4.598	-4.374	0.216
Mol-8	-4.553	-4.355	0.244

According to the computed results pristine has a HOMO-LUMO energy gap of 0.216 eV while the modeled molecules (Mol-1 to Mol-8) have energy gap from 0.201 to 0.244 eV, which is not so different from the pristine molecule.

#### 4.4 Electronic properties

The electronic characteristics of molecules are determined by the energy gap (E<sub>gap</sub>) between the highest occupied molecular orbital (HOMO) and the lowest unoccupied molecular orbital (LUMO) energy levels (as shown in Table). Smaller E<sub>gap</sub> values are more favorable for electronic properties. The average E<sub>gap</sub> that was obtained through this study is 0.22 eV; however, the E<sub>gap</sub> that was determined for all of the molecules that belong to M1-M8 ranged from 0.201 to 0.244 eV. In the molecule Mol-2 in which two number of carbon chains are attached between bigger donating agent at the D1 part of D1-A-D2 to assist the conduction, the result demonstrates that the E<sub>gap</sub> with the minimum value, 0.201 eV, is present. HOMO LUMO energy values, and their energy gap were listed in Table 4.6.

Table 4.3. HOMO-LUMO energy values and Energy gap values of Pristine and M1-M8

Structure	HOMO (eV)	LUMO (eV)	Energy gap (eV)
Pristine	-4.619	-4.404	0.216
Mol-1	-4.544	-4.319	0.224
Mol-2	-4.558	-4.357	0.201
Mol-3	-4.507	-4.27	0.237
Mol-4	-4.532	-4.319	0.213
Mol-5	-4.606	-4.404	0.216
Mol-6	-4.59	-4.392	0.214
Mol-7	-4.598	-4.374	0.216
Mol-8	-4.553	-4.355	0.244

## 4.5 Electronic Transition and Absorption spectra

The electronic transition data was obtained for all the modelled geometries. This method was used to determine their theoretical absorption  $\lambda_{\text{max}}$  (nm), vertical excitation energy  $E_{\text{tr}}$  (eV), oscillator strength (O.S), and molecular orbital character (MO/character). The calculation of the excitation configuration is presented in Table 4.8 As a result of the findings, every stage of the electronic excitation was revealed to be a  $\pi$ - $\pi^*$  process, successfully transferring charge within the molecules. The wavelength range of 400-800nm is significant for photovoltaic applications due to the fact that radiation with longer wavelengths, such as radio waves and microwaves does not possess sufficient energy to generate electricity in a solar cell. We have acquired a range of wavelengths spanning from 4113.27 to 13992.63 nm, and their Oscillator strength values 0.015 to 0.178 including the UV/Vis to Infrared regions of the electromagnetic spectrum, with only a small number of compounds exhibiting absorption.

Table 4.4. The absorption  $\lambda_{\text{max}}$  (nm), oscillator strength (O.S), of Pristine and M1-M8

Structures	Wavelength (nm)	Oscillator strength
Pristine	9960.25	0.030
Mol-1	6455.27	0.073
Mol-2	8989.01	0.034
Mol-3	4968.3	0.125
Mol-4	13992.63	0.015
Mol-5	10982.7	0.024
Mol-6	10826.5	0.025
Mol-7	4568.6	0.143
Mol-8	4113.27	0.178

The absorption (UV/Vis) spectra of the pristine structure and M1-M8 is shown in table 4.6. The carbon chains serve as conjugated linkages connecting the donor and acceptor. Increased carbon chain length enhances the total correlation length of the molecule, hence influencing the electrical interaction between the donor and acceptor. A specific degree of conjugation would be present in the molecule if there was no carbon chain connecting the donors. With a rise in the number of carbon chains, the length of conjugation is expected to grow. Increased conjugation can lead to redshifts in the absorption spectra. Electronic transitions begin with  $\pi$ - $\pi^*$  transitions of donor and acceptor units. The absorption of the pristine structure molecule is 9960.25 nm. The absorption of the M4 is higher than the M1 (6455.27nm), M2 (8989.01nm), and M3 (4968.3 nm),M5 (10982.7 nm), M6 (10826.5) ,M7 (4568.6) , and Mol (4113.27).The Absorption of all the molecules has a significant value Specialty Mol-4(13992.63 nm), causing it to shift from the ultraviolet (UV) to the infrared region of the electromagnetic spectrum. This property makes it potentially useful in solar cells, as it can modify the spectrum and enable up-conversion. By combining fullerene with other inorganic semiconductors, this phenomenon has been observed in the development of next-generation solar cells that harness infrared rays.

Table 4.5. Theoretical absorption  $\lambda_{\text{max}}$  (nm), vertical excitation energy  $E_{\text{tr}}$  (eV), oscillator strength (O.S), and molecular orbital character (MO/character) of M1-M8 optimized geometries

Mol.	$\lambda_{\text{ab}}$ (nm)	$E_{\text{tr}}$ (eV)	O. S	MO/characters
Pristine	9960.25	0.1245	0.0303	H→L (1.98264)
	1899.88	0.6526	0.0336	H-1→L (0.70310)
	1451.76	0.8540	0.0027	H→L+1 (0.70638)
M-1	6455.27	0.1921	0.0730	H→L (1.62815)
	1916.60	0.6469	0.0222	H-1→L (0.70518)
	1804.91	0.6869	0.0002	H→L+1 (0.70692)
M-2	8989.01	0.1379	0.0343	H→L (-0.14701), H+1→L (-1.77916)
	2265.71	0.5472	0.0876	H+1→L (-0.35515)
	1701.34	0.7287	0.0001	H-1→L+1(0.70688)
M-3	4968.30	0.2496	0.1256	H→L (1.44761)
	1986.37	0.6242	0.0000	H→L+1(0.70698)
	1862.08	0.6658	0.0309	H-1→L (0.70658)
M-4	13992.63	0.0886	0.0153	H→L (2.30604)
	2317.62	0.5350	0.0312	H-1→L (0.70283)
	2028.00	0.6114	0.0000	H→L+1(0.70704)
M-5	10982.70	0.1129	0.0248	H→L (2.06427)
	1915.70	0.6472	0.0383	H-1→L (0.70291),
	1256.04	0.9871	0.0011	H→L+1 (0.59176), H→L+2 (-0.37835)
M-6	10826.57	0.1145	0.0254	H→L (2.04984)
	1967.66	0.6301	0.0351	H-1→L (0.70297)
	1257.11	0.9863	0.0007	H→L+1 (0.44947), H→L+2 (0.53858)
M-7	4568.65	0.2714	0.1439	H→L (1.39990)
	1603.39	0.7733	0.0362	H-1→L (0.70608)
	1243.78	0.9968	0.0003	H→L+1(0.63207), H→L+2(0.13292), H→L+4 (0.27752)
M-8	4113.27	0.3014	0.1775	H→L (1.33466)
	1604.75	0.7726	0.0419	H-1→L (0.70653)
	1246.22	0.9949	0.0004	H→L+1(0.68492), H→L+2 (-0.14097)

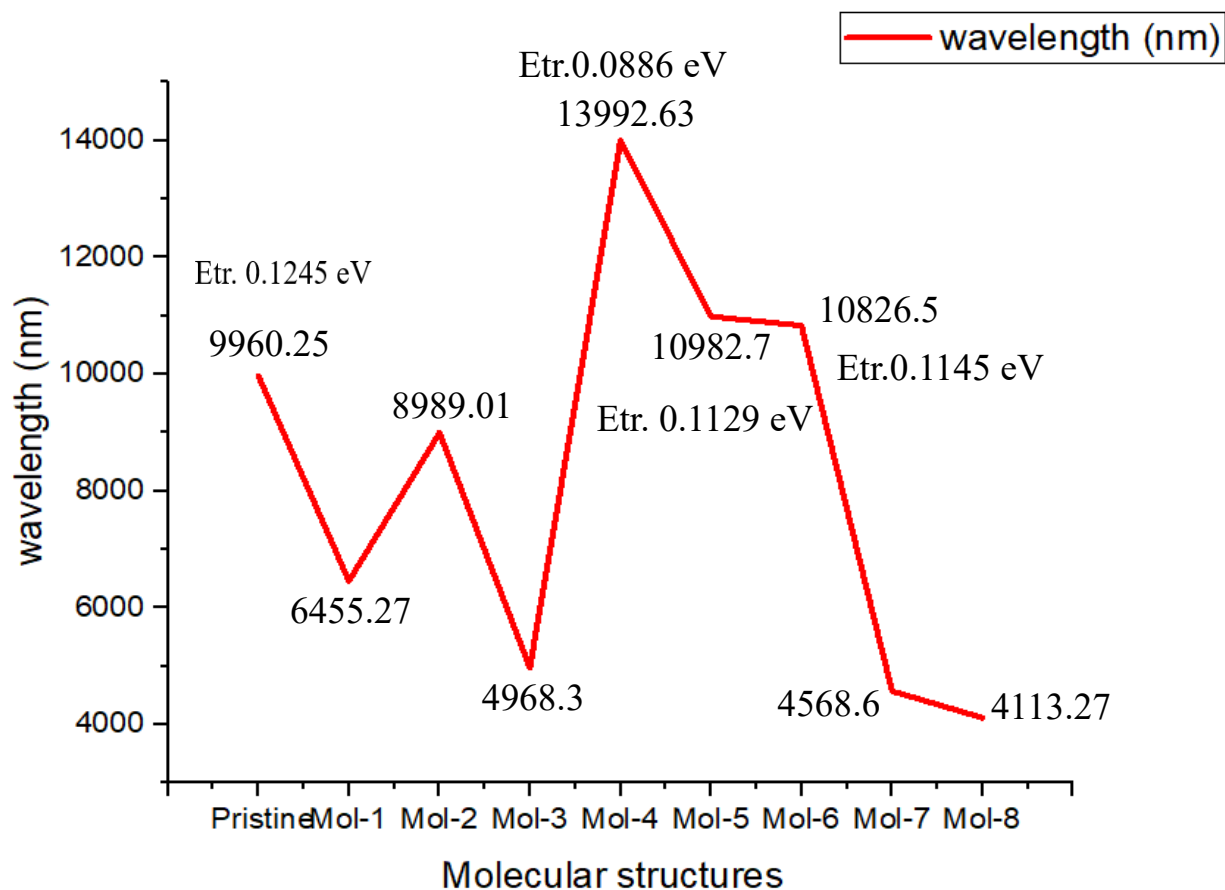


Figure 4.6. The Graphical representation UV-Vis spectrum of Of M1-M8

#### 4.6 Photovoltaic properties

The photovoltaic performance of the studied compounds was evaluated by calculating the open circuit voltage  $V_{oc}$  (eV) and  $\alpha$  (eV) of M1-M8 of D-A-D materials. Solar cells may generate their maximum voltage without a load at the open-circuit voltage. It depends on the energy levels of the donor material's HOMO and the acceptor material's LUMO. The theoretical values of  $V_{oc}$  and  $\alpha$  were calculated using the equation 1 and 2 below:

$$V_{oc} = |E_{HOMO}(\text{donor})| - |E_{LUMO}(\text{acceptor})| - 0.3 \quad \text{equation-1}$$

$$\alpha = |\text{ELUMO (acceptor)}| - |\text{ELUMO (donor)}| \quad \text{equation-2}$$

The energy difference is often strongly associated with the energy difference between the highest occupied molecular orbital (HOMO) of the donor and the lowest unoccupied molecular orbital (LUMO) of the acceptor inside a molecule. These values may be found in Table 4.10. The findings shown that the Voc may be adjusted by manipulating the energy gap correlation between the donor and acceptor components. The Voc and  $\alpha$  values proposed investigated M1-M8 of D-A-D materials for electron ejection, rendering them well-suited for bulk heterojunction and enhancing their viability for utilisation in solar cell applications

Table 4.6. Showing the relationship of HOMO, LUMO, energy gap, Voc and  $\alpha$  of M1-M8

S No.	Structures	$E_{\text{HOMO}}$ (eV)	$E_{\text{LUMO}}$ (eV)	$E_{\text{gap}}$ (eV)	Voc (eV)	$\alpha$ (eV)
1	Pristine	-4.619	-4.404	0.22	0.62	-0.70
2	Mol-1	-4.544	-4.319	0.22	0.54	-0.62
3	Mol-2	-4.558	-4.357	0.20	0.56	-0.66
4	Mol-3	-4.507	-4.270	0.24	0.51	-0.57
5	Mol-4	-4.532	-4.319	0.21	0.53	-0.62
6	Mol-5	-4.606	-4.392	0.21	0.61	-0.69
7	Mol-6	-4.590	-4.374	0.22	0.59	-0.67
8	Mol-7	-4.598	-4.355	0.24	0.60	-0.65
9	Mol-8	-4.553	-4.303	0.25	0.55	-0.60

In this this table the Voc value is contingent upon the highest occupied molecular orbital (HOMO) level of the donor and the lowest unoccupied molecular orbital (LUMO) level of the acceptor. The range of the variable "Voc" is from 0.51 to 0.62, with an average value of 0.56. The range of the variable " $\alpha$ " is from -0.57 to -0.70, with an average value of -0.64. The Voc values indicate that this range is adequate for efficient electron ejection, making them highly appropriate for bulk

heterojunctions and hence more practical for usage in solar cells. Mol-3 possesses the most significant band gap, measuring 0.24 eV. This characteristic has the potential to facilitate the absorption of photons with greater energy levels. Mol-2 exhibits a comparatively narrow band gap of 0.20 eV. It is evident that Mol-1 possesses the second-highest VOC (Volatile Organic Compound) value, measuring 0.54 eV, whereas Pristine exhibits the greatest VOC value of 0.6 eV. Therefore, Pristine possesses the greatest open-circuit voltage out of all the chemical structure.

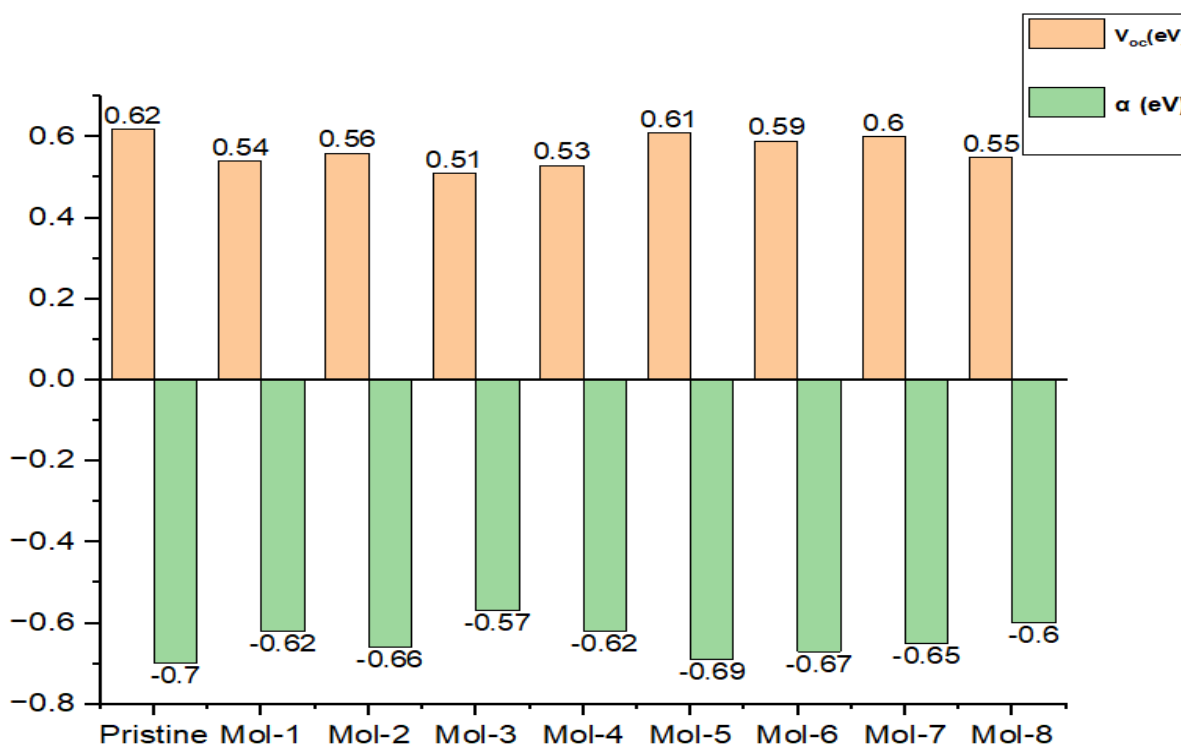


Figure 4.7 Graphical representation of  $V_{oc}$  (eV) and  $\alpha$  (eV) of Mol-1 to Mol-8

These computed results were also compared with the values reported in the literature. Up till now, the lowest band gap energy reported was 1.70 eV which is higher than the band gap energy reported here for pristine is 0.22 eV[85]. Also, the electronic transitions are favorable relative to the reported in literature. Similarly, the photovoltaic properties of our molecules are much better than many reported molecules. With a  $V_{oc}$  range of reported data 0.24 to 2.57 (average 1.29), electron ejection

in photovoltaic applications is flexible[114]. We found a smaller Voc range of 0.51–0.62 (average 0.56) that is still sufficient for solar cells.

The investigation of carbon chain between the donor-acceptor and acceptor donor parts of organic materials for PV cells was a unique study, never reported in the literature. Based on our study we can conclude that the carbon chain can affect the efficiency of PV cells when attached with the donor or acceptor parts but has no effect when added between the donor and acceptor units.

# Chapter 5

## Discussion

Solar energy is widely recognized as a plentiful and environmentally friendly form of power, prompting researchers to devote considerable resources towards its use in the production of electricity. One popular method is photovoltaics, which utilize the photovoltaic effect to convert solar energy into electricity. Photovoltaics can be classified into two distinct categories: inorganic and organic. Significant advancements have been made in the field of inorganic solar cells over the course of the past several decades. The conversion of solar energy into electrical energy using photovoltaic cells is currently one of the most exciting research challenges. Organic photovoltaic (OPV) cells are in high demand for photovoltaic applications because of their mechanical flexibility, affordability, ease of production, and lightweight nature. The research has primarily focused on D-A-D (Donor-Acceptor-Donor) photovoltaic cells, extensively investigating the properties of Donor 1 units, Acceptor units, and Donor 2 units. Donor-1(triphenylamine) and (4,7-dimethyl- [1,2,5] oxadiazolo[3,4-c] pyridine), as well as the acceptor and donor-2 (2,5 dimethylthiophene) units is used as organic materials. According to the reported literature it has been observed that attaching carbon chains to both the Donor and Acceptor units can have positive effects on the performance of these organic photovoltaic material. Significant study gap exists about the impact of the carbon chain that bridges between D-A and A-D units of organic material have any positive impact or not. So, in this research all model geometries of the optimized geometry of Pristine structure and its derivatives in which we increased the carbon chain from 1-4 between donor-acceptor and acceptor donor parts. Comparing the Relative energies, it has been

observed that ~32.8 eV energy is required to add the methyl group between the D-A and A-D parts. This shows that the increase in carbon chain is an endothermic reaction.

The electronic characteristics of molecules are determined by the energy gap (E<sub>gap</sub>) between the highest occupied molecular orbital (HOMO) and the lowest unoccupied molecular orbital (LUMO) energy levels. Smaller E<sub>gap</sub> values are more favorable for electronic properties. Our results on the energy gap (E<sub>gap</sub>) differ significantly from the ones that have been published. According to the study that was released, the average E<sub>gap</sub> is 2.1 eV, and it varies widely across molecules, ranging from 0.227 to 2.808 eV. This points to a large variety in the electrical characteristics of these compounds. Our findings, on the other hand, reveal a considerably more condensed picture, with an average E<sub>gap</sub> of a mere 0.22 eV and a range for molecules M1-M8 that is tightly packed between 0.201 and 0.244 eV. The average E<sub>gap</sub> that was obtained through this study is 0.22 eV; however, the E<sub>gap</sub> that was determined for all of the molecules that belong to M1-M8 ranged from 0.201 to 0.244 eV.

Table 4.7. Energy Gap Values of Pristine and Mol1-Mol8

Structure	Energy Gap (eV)
Pristine	0.216
Mol-1	0.224
Mol-2	0.201
Mol-3	0.237
Mol-4	0.213
Mol-5	0.216
Mol-6	0.214
Mol-7	0.216
Mol-8	0.244

The photovoltaic wavelength of 400-800nm is important since microwaves and radio waves lack the energy to generate power from a solar cell. We found wavelengths of already reported organic material from 491.93 to 5351.13 nm, when carbon chain attached to the donor and acceptor units spanning UV/Vis to Infrared (few molecules). Data reveals that benzothiadiazide as acceptor has a shorter wavelength than methyl/alkyl groups. When the absorption spectra of the molecules calculated the wavelength of the molecules increases with the addition of four carbon atoms between the D-A and A-D. Pristine has a wavelength of 9960nm. The energy and wavelength have an inverse relation. For the solar cell energy, we need longer wavelength. Mol 413992.63nm has smaller excitation energy  $E_{tr}$ . 0.0886 eV.

The photovoltaic performance of the studied compounds was evaluated by calculating the open circuit voltage  $V_{oc}$  (eV) and  $\alpha$  (eV) of M1-M8 of D-A-D materials. Solar cells may generate their maximum voltage without a load at the open-circuit voltage. It depends on the energy levels of the donor material's HOMO and the acceptor material's LUMO. Compared to reported data, our  $V_{oc}$  readings are significantly different. With a  $V_{oc}$  range of reported data 0.24 to 2.57 (average 1.29), electron ejection in photovoltaic applications is flexible. We found a smaller  $V_{oc}$  range of 0.51–0.62 (average 0.56) that is still sufficient for solar cells. The  $\alpha$  ranges from -0.70 to 1.67 (average 0.56), while our results indicate a narrower yet more negative range from -0.57 to -0.70 (average -0.64), indicating unique electrical characteristics in the materials investigated.



# Chapter 6

## Conclusion

In this study, we investigated the "Design and Analysis of Donor-Acceptor-Donor Parts of Organic Materials for Photovoltaic Cells" with a specific focus on the effect of strategic modulation of carbon chain lengths between the donor-1(triphenylamine) and acceptor (4,7-dimethyl- [1,2,5] oxadiazolo[3,4-c] pyridine), as well as the acceptor and donor-2 (2,5 dimethylthiophene) units. The performance of designed D-A-D molecules was evaluated by calculating structural, electronic, optical, and absorption properties using DFT-B3LYP/6-31G(d) levels. According to computed data for the model geometries Mol-1 to Mol-8, the addition of methyl groups led to a considerable increase in relative energy. The assessment of HOMO-LUMO energy gaps indicated that of pristine is 0.216 eV. The HOMO-LUMO of modeled structures has almost like the same values their average energy gap is 0.22 eV. When the absorption spectra of the molecules calculated the wavelength of the molecules increases with the addition of four carbon atoms. Pristine has wavelength 9960nm. The energy and wavelength have inverse relation. For the solar cell energy, we need longer wavelength. Mol 413992.63nm have smaller excitation energy  $E_{tr}$  0.0886 eV. The evaluation of photovoltaic efficacy comprised various parameters, one of which was open circuit voltage (Voc). The open-circuit voltage (Voc) has decreased, with "Voc" ranging from 0.51 to 0.62, and exhibiting an average value of 0.56 eV. The pristine structure exhibited a Voc maximum of 0.62 electron volts (eV). There is no much impact on the length of carbon chain between the donor-acceptor and acceptor- donor units of D1-A-D2 organic materials on various

## *Conclusion and Future Perspective*

properties, including relative energy values, electronic properties, absorption characteristics (wavelength range), and photovoltaic properties.

## **Future Perspective**

In the future, we will concentrate on developing unique D-A-D designs for organic photovoltaic solar cells by adding various functional groups and substituents into the donor and acceptor moieties. We intend to optimize the synthesis of these materials for scale manufacturing, working closely with industry partners to create low-cost fabrication processes. Efforts will be made to investigate the effect of substituents on photovoltaic characteristics and to improve efficiency using improved device topologies. Furthermore, we will focus on examining stability difficulties, developing future technologies, and integrating D-A-D solar cells into mainstream markets. The dedication to ecologically safe disposal techniques, recyclability, and sustainable practices will underpin our approach to promoting this potential renewable energy technology.

# References

1. Mazzio, K.A. and C.K.J.C.S.R. Luscombe, *The future of organic photovoltaics*. 2015. **44**(1): p. 78-90.
2. Bagher, A.M.J.I.J.R.S.E., *Comparison of organic solar cells and inorganic solar cells*. 2014. **3**(3): p. 53-58.
3. Blandford, R. and M.J.A.N. Watkins, *This month in physics history: April 25, 1954: bell labs demonstrates the first practical silicon solar cell*. 2009. **18**(4): p. 2.
4. Green, M.A.J.P.i.P.R. and Applications, *Corrigendum to 'Solar cell efficiency tables (version 46)'* [*Prog. Photovolt: Res. Appl.* 2015; 23: 805–812]. 2015. **23**(9): p. 1202-1202.
5. Kampas, F.J. and M.J.T.J.o.P.C. Gouterman, *Porphyrin films. 3. Photovoltaic properties of octaethylporphine and tetraphenylporphine*. 1977. **81**(8): p. 690-695.
6. Winder, C., et al., *Sensitization of low bandgap polymer bulk heterojunction solar cells*. 2002. **403**: p. 373-379.
7. Zhang, F., et al., *High photovoltage achieved in low band gap polymer solar cells by adjusting energy levels of a polymer with the LUMOs of fullerene derivatives*. 2008. **18**(45): p. 5468-5474.
8. Pan, Z., et al., *Graphene-based functional materials for organic solar cells*. 2012. **2**(6): p. 814-824.
9. Gupta, A., et al., *The effect of direct amine substituted push–pull oligothiophene chromophores on dye-sensitized and bulk heterojunction solar cells performance*. 2013. **69**(17): p. 3584-3592.

10. Tang, C.W.J.A.p.l., *Two-layer organic photovoltaic cell*. 1986. **48**(2): p. 183-185.
11. Yu, G., et al., *Polymer photovoltaic cells: enhanced efficiencies via a network of internal donor-acceptor heterojunctions*. 1995. **270**(5243): p. 1789-1791.
12. Timilsina, G.R., et al., *Solar energy: Markets, economics and policies*. 2012. **16**(1): p. 449-465.
13. Singh, G., et al., *Exergy and thermoeconomic analysis of cream pasteurisation plant*. 2019. **137**: p. 1381-1400.
14. Pandey, A.K., et al., *Energy and exergy performance evaluation of a typical solar photovoltaic module*. 2015. **19**(suppl. 2): p. 625-636.
15. Elhadidy, M.A.J.R.e., *Performance evaluation of hybrid (wind/solar/diesel) power systems*. 2002. **26**(3): p. 401-413.
16. McFarland, E.J.E. and E. Science, *Solar energy: setting the economic bar from the top-down*. 2014. **7**(3): p. 846-854.
17. Lorenzo, E., *Solar electricity: engineering of photovoltaic systems*. 1994: Progensa.
18. Anderson, D., *Clean Electricity from Photovoltaics, eds*. 2001, MD Archer and RD Hill (London: Imperial College Press, 2001).
19. Singh, G.K.J.E., *Solar power generation by PV (photovoltaic) technology: A review*. 2013. **53**: p. 1-13.
20. Dasgupta, A., *Vertical Solar Panel: An Innovative approach Towards mitigating Energy Crisis situation of Urban India*.
21. Villalva, M.G., J.R. Gazoli, and E.J.I.T.o.p.e. Ruppert Filho, *Comprehensive approach to modeling and simulation of photovoltaic arrays*. 2009. **24**(5): p. 1198-1208.

22. Patel, M., et al., *Carrier transport and working mechanism of transparent photovoltaic cells*. 2022. **26**: p. 101344.
23. Tyagi, V., et al., *Progress in solar PV technology: Research and achievement*. 2013. **20**: p. 443-461.
24. Jäger-Waldau, A.J.P.O.o.t.E.U.L., *PV status report 2019*. 2019: p. 7-94.
25. Nayak, P.K., et al., *Photovoltaic efficiency limits and material disorder*. 2012. **5(3)**: p. 6022-6039.
26. McCann, M.J., et al., *A review of thin-film crystalline silicon for solar cell applications. Part 1: Native substrates*. 2001. **68(2)**: p. 135-171.
27. El Char, L., N.J.R. El Zein, and s.e. reviews, *Review of photovoltaic technologies*. 2011. **15(5)**: p. 2165-2175.
28. Gorter, T. and A.H.J.A.e. Reinders, *A comparison of 15 polymers for application in photovoltaic modules in PV-powered boats*. 2012. **92**: p. 286-297.
29. Imamzai, M., et al. *A review on comparison between traditional silicon solar cells and thin-film CdTe solar cells*. in *Proceedings of National Graduate Conference (Nat-Grad)*. 2012.
30. Williams, B., et al., *Challenges and prospects for developing CdS/CdTe substrate solar cells on Mo foils*. 2014. **124**: p. 31-38.
31. Kabir, M.I., et al., *Amorphous silicon single-junction thin-film solar cell exceeding 10% efficiency by design optimization*. 2012. **2012**.
32. Johansson, A., R. Gottschalg, and D. Infield. *Modelling shading on amorphous silicon single and double junction modules*. in *3rd World Conference on Photovoltaic Energy Conversion, 2003. Proceedings of*. 2003. IEEE.

33. Yunaz, I.A., A. Yamada, and M.J.J.J.o.A.P. Konagai, *Theoretical analysis of amorphous silicon alloy based triple junction solar cells*. 2007. **46**(12L): p. L1152.
34. Andorka, F.J.S.P.W.A.f.t.o.o., *CIGS Solar Cells, Simplified*. 2014. **16**.
35. Srinivas, B., et al., *Review on present and advance materials for solar cells*. 2015. **3**(2015): p. 178-182.
36. Contreras, M.A., M.J. Romero, and R.J.T.S.F. Noufi, *Characterization of Cu (In, Ga) Se<sub>2</sub> materials used in record performance solar cells*. 2006. **511**: p. 51-54.
37. Report, E.P.I.A.J.E., *Global market outlook for photovoltaics 2013-2017*. 2013.
38. Würfel, P. and U. Würfel, *Physics of solar cells: from basic principles to advanced concepts*. 2016: John Wiley & Sons.
39. Dimitrijević, S., *Principles of semiconductor devices*. 2006: Oxford University Press. USA.
40. Bertolli, M.J.D.o.P., University of Tennessee, *Solar Cell Materials. Course: Solid State II*. 2008.
41. Manna, T.K. and S.M. Mahajan. *Nanotechnology in the development of photovoltaic cells*. in *2007 International Conference on Clean Electrical Power*. 2007. IEEE.
42. Saga, T.J.n.a.m., *Advances in crystalline silicon solar cell technology for industrial mass production*. 2010. **2**(3): p. 96-102.
43. Sharma, S., et al., *Solar cells: in research and applications—a review*. 2015. **6**(12): p. 1145.
44. Deb, S.K.J.R.e., *Recent developments in high efficiency photovoltaic cells*. 1998. **15**(1-4): p. 467-472.
45. Choubey, P., et al., *A review: Solar cell current scenario and future trends*. 2012. **4**(8).

46. Leroy, F., *A century of Nobel Prize recipients: chemistry, physics, and medicine*. 2003: CRC Press.
47. Mayer, A.C., et al., *Polymer-based solar cells*. 2007. **10**(11): p. 28-33.
48. Wudl, F. and G. Srdanov, *Conducting polymer formed of poly (2-methoxy, 5-(2'-ethyl-hexyloxy)-p-phenylenevinylene)*. 1993, Google Patents.
49. Milliron, D.J., I. Gur, and A.P.J.M.b. Alivisatos, *Hybrid organic–nanocrystal solar cells*. 2005. **30**(1): p. 41-44.
50. Yuan, Y., et al., *Photovoltaic switching mechanism in lateral structure hybrid perovskite solar cells*. 2015. **5**(15): p. 1500615.
51. Grätzel, M.J.J.o.p. and p.C.P. Reviews, *Dye-sensitized solar cells*. 2003. **4**(2): p. 145-153.
52. Nazeeruddin, M.K., E. Baranoff, and M.J.S.e. Grätzel, *Dye-sensitized solar cells: A brief overview*. 2011. **85**(6): p. 1172-1178.
53. Ahmad, I., et al., *Carbon nanomaterial based counter electrodes for dye sensitized solar cells*. 2014. **102**: p. 152-161.
54. Rand, B.P., et al., *Solar cells utilizing small molecular weight organic semiconductors*. 2007. **15**(8): p. 659-676.
55. Freiman, S.W. and L.D.J.A.C.S.B. Madsen, *Issues of scarce materials in the United States*. 2012. **91**(3): p. 40-45.
56. Xiao, S., S.J.C.r.i.s.s. Xu, and m. sciences, *High-efficiency silicon solar cells—materials and devices physics*. 2014. **39**(4): p. 277-317.
57. Vilkmann, M., et al., *Fully roll-to-roll processed organic top gate transistors using a printable etchant for bottom electrode patterning*. 2015. **20**: p. 8-14.

58. Ragoussi, M.-E. and T.J.C.C. Torres, *New generation solar cells: concepts, trends and perspectives*. 2015. **51**(19): p. 3957-3972.
59. Petritsch, K., *Organic solar cell architectures*. 2000: na.
60. Chang, C.Y., et al., *Combination of molecular, morphological, and interfacial engineering to achieve highly efficient and stable plastic solar cells*. 2012. **24**(4): p. 549-553.
61. Zhang, S., et al., *Organic solar cells with 2-Thenylmercaptan/AU self-assembly film as buffer layer*. 2011. **95**(3): p. 917-920.
62. Fan, X., et al., *Efficient polymer solar cells based on poly (3-hexylthiophene): indene-C70 bisadduct with a MoO<sub>3</sub> buffer layer*. 2012. **22**(3): p. 585-590.
63. Kaur, N., et al., *Organic materials for photovoltaic applications: Review and mechanism*. 2014. **190**: p. 20-26.
64. Nicholson, M., et al., *Phthalocyanines: properties and applications*. 1993. **3**.
65. McKeown, N.B., *Phthalocyanine materials: synthesis, structure and function*. 1998: Cambridge university press.
66. De La Torre, G., et al., *Phthalocyanines: synthesis, supramolecular organization, and physical properties*. 2001: p. 1-111.
67. Hong, Z., Z. Huang, and X.J.C.P.L. Zeng, *Investigation into effects of electron transporting materials on organic solar cells with copper phthalocyanine/C60 heterojunctions*. 2006. **425**(1-3): p. 62-65.
68. Claessens, C.G., D. González-Rodríguez, and T.J.C.r. Torres, *Subphthalocyanines: singular nonplanar aromatic compounds synthesis, reactivity, and physical properties*. 2002. **102**(3): p. 835-854.

69. Wang, Y., D. Gu, and F.J.p.s.s. Gan, *Optical recording properties of a novel subphthalocyanine thin film*. 2001. **186**(1): p. 71-77.
70. Mutolo, K.L., et al., *Enhanced open-circuit voltage in subphthalocyanine/C60 organic photovoltaic cells*. 2006. **128**(25): p. 8108-8109.
71. Takahashi, K., et al., *Enhanced photocurrent in Al/porphyrin Schottky barrier cell with heterodimer consisting of metal-free porphyrin and zinc porphyrin*. 1999. **103**(23): p. 4868-4875.
72. Fischer, M.K., et al., *Functionalized dendritic oligothiophenes: ruthenium phthalocyanine complexes and their application in bulk heterojunction solar cells*. 2009. **131**(24): p. 8669-8676.
73. Oku, T., et al., *Fabrication and characterization of fullerene/porphyrin bulk heterojunction solar cells*. 2010. **71**(4): p. 551-555.
74. Perzon, E., et al., *Design, synthesis and properties of low band gap polyfluorenes for photovoltaic devices*. 2005. **154**(1-3): p. 53-56.
75. Guan, Z.-L., et al., *Direct determination of the electronic structure of the poly (3-hexylthiophene): phenyl-[6, 6]-C61 butyric acid methyl ester blend*. 2010. **11**(11): p. 1779-1785.
76. Ishii, T., et al., *Fullerene C 60 exhibiting a strong intermolecular interaction in a cocrystallite with C 4 symmetrical cobalt tetrakis (di-tert-butylphenyl) porphyrin*. 2001(20): p. 2975-2980.
77. Hummelen, J.C., et al., *Preparation and characterization of fulleroid and methanofullerene derivatives*. 1995. **60**(3): p. 532-538.

78. Liu, C., et al., *Low bandgap semiconducting polymers for polymeric photovoltaics*. 2016. **45**(17): p. 4825-4846.
79. Guo, X., M. Baumgarten, and K.J.P.i.P.S. Müllen, *Designing  $\pi$ -conjugated polymers for organic electronics*. 2013. **38**(12): p. 1832-1908.
80. Müllen, K. and W.J.J.o.t.A.C.S. Pisula, *Donor–acceptor polymers*. 2015, ACS Publications. p. 9503-9505.
81. Günes, S., H. Neugebauer, and N.S.J.C.r. Sariciftci, *Conjugated polymer-based organic solar cells*. 2007. **107**(4): p. 1324-1338.
82. Thompson, B.C. and J.M.J.A.c.i.e. Fréchet, *Polymer–fullerene composite solar cells*. 2008. **47**(1): p. 58-77.
83. Dennler, G., M.C. Scharber, and C.J.J.A.m. Brabec, *Polymer–fullerene bulk-heterojunction solar cells*. 2009. **21**(13): p. 1323-1338.
84. Cheng, Y.-J., S.-H. Yang, and C.-S.J.C.r. Hsu, *Synthesis of conjugated polymers for organic solar cell applications*. 2009. **109**(11): p. 5868-5923.
85. Yassin, A., et al., *A donor–acceptor–donor (D–A–D) molecule based on 3-alkoxy-4-cyanothiophene and dithienopyrrole units as active material for organic solar cells*. 2012. **36**(11): p. 2412-2416.
86. Silvestri, F., et al., *Efficient squaraine-based solution processable bulk-heterojunction solar cells*. 2008. **130**(52): p. 17640-17641.
87. Mayerhöffer, U., et al., *Outstanding Short-Circuit Currents in BHJ Solar Cells Based on NIR-Absorbing Acceptor-Substituted Squaraines*. 2009. **48**(46): p. 8776-8779.

88. Mikroyannidis, J., et al., *Low band gap conjugated small molecules containing benzobisthiadiazole and thienothiadiazole central units: synthesis and application for bulk heterojunction solar cells*. 2011. **21**(12): p. 4679-4688.
89. Marx, D. and J. Hutter, *Ab initio molecular dynamics: basic theory and advanced methods*. 2009: Cambridge University Press.
90. Esselman, B.J. and N.J.J.J.o.C.E. Hill, *Integration of computational chemistry into the undergraduate organic chemistry laboratory curriculum*. 2016. **93**(5): p. 932-936.
91. Jensen, F., *Introduction to computational chemistry*. 2017: John wiley & sons.
92. Rapaport, D.C., *The art of molecular dynamics simulation*. 2004: Cambridge university press.
93. Bao, G. and S.J.N.m. Suresh, *Cell and molecular mechanics of biological materials*. 2003. **2**(11): p. 715-725.
94. Lewars, E.G., et al., *Introduction to Quantum Mechanics in Computational Chemistry*. 2016: p. 101-191.
95. Chen, M., et al., *Ab initio theory and modeling of water*. 2017. **114**(41): p. 10846-10851.
96. North, A., et al., *A semi-empirical method of absorption correction*. 1968. **24**(3): p. 351-359.
97. Brandbyge, M., et al., *Density-functional method for nonequilibrium electron transport*. 2002. **65**(16): p. 165401.
98. Chigo Anota, E., H. Hernández Cocoltzi, and E.J.T.E.P.J.D. Rubio Rosas, *LDA approximation based analysis of the adsorption of O<sub>3</sub> by boron nitride sheet*. 2011. **63**: p. 271-273.

99. Vasić, D., et al., *Systematic DFT-GGA study of hydrogen adsorption on transition metals*. 2011. **85**: p. 2373-2379.
100. Fraas, L.M. and M.J. O'Neill, *History of solar cell development*, in *Low-cost solar electric power*. 2023, Springer. p. 1-12.
101. Kim, M.-S., *Understanding organic photovoltaic cells: Electrode, nanostructure, reliability, and performance*. 2009: University of Michigan.
102. Sivula, K. and R.J.N.R.M. Van De Krol, *Semiconducting materials for photoelectrochemical energy conversion*. 2016. **1**(2): p. 1-16.
103. Wolf, M. and H.J.S.C. Rauschenbach, *Series resistance effects on solar cell measurements*. 1976: p. 146-170.
104. Green, M.A. *Photovoltaics: coming of age*. in *IEEE Conference on Photovoltaic Specialists*. 1990. IEEE.
105. Markvart, T., *Solar electricity*. Vol. 6. 2000: John Wiley & Sons.
106. Irfan, A. and A.G.J.J.o.m.m. Al-Sehemi, *Quantum chemical study in the direction to design efficient donor-bridge-acceptor triphenylamine sensitizers with improved electron injection*. 2012. **18**: p. 4893-4900.
107. Lee, J.W., Y.S. Choi, and W.H.J.O.E. Jo, *Diketopyrrolopyrrole-based small molecules with simple structure for high VOC organic photovoltaics*. 2012. **13**(12): p. 3060-3066.
108. Ni, W., et al., *Open-circuit voltage up to 1.07 V for solution processed small molecule based organic solar cells*. 2014. **15**(10): p. 2285-2294.
109. Dimitrov, S.D. and J.R.J.C.o.M. Durrant, *Materials design considerations for charge generation in organic solar cells*. 2014. **26**(1): p. 616-630.

110. Hori, T., et al., *Solution processable organic solar cell based on bulk heterojunction utilizing phthalocyanine derivative*. 2010. **3**(10): p. 101602.
111. Du, C., et al., *Organic solar cells using Tin (II) phthalocyanine as donor material*. 2011. **12**: p. 519-524.
112. Williams, G., et al., *Renewed interest in metal phthalocyanine donors for small molecule organic solar cells*. 2014. **124**: p. 217-226.
113. Salzman, R.F., et al., *The effects of copper phthalocyanine purity on organic solar cell performance*. 2005. **6**(5-6): p. 242-246.
114. Kumar, P., et al., *Improving the photovoltaic parameters of organic solar cell using soluble copper phthalocyanine nanoparticles as a buffer layer*. 2013. **53**(1S): p. 01AB06.
115. Beaumont, N., et al., *Boron subphthalocyanine chloride as an electron acceptor for high-voltage fullerene-free organic Photovoltaics*. 2012. **22**(3): p. 561-566.
116. Ren, Y., et al., *Utilizing non-conjugated small-molecular tetrasodium iminodisuccinate as electron transport layer enabled improving efficiency of organic solar cells*. 2022. **129**: p. 112520.
117. Song, Q., et al., *Role of buffer in organic solar cells using C60 as an acceptor*. 2007. **90**(7).
118. Pandey, R., et al., *Efficient organic photovoltaic cells based on nanocrystalline mixtures of boron subphthalocyanine chloride and C60*. 2012. **22**(3): p. 617-624.
119. He, Y. and Y.J.P.c.c.p. Li, *Fullerene derivative acceptors for high performance polymer solar cells*. 2011. **13**(6): p. 1970-1983.
120. Zhang, F., et al., *Influence of PC60BM or PC70BM as electron acceptor on the performance of polymer solar cells*. 2012. **97**: p. 71-77.

121. He, Y., et al., *High-yield synthesis and electrochemical and photovoltaic properties of indene-C70 bisadduct*. 2010. **20**(19): p. 3383-3389.
122. Sun, Y., et al., *Efficiency enhancement of polymer solar cells based on poly (3-hexylthiophene)/indene-C70 bisadduct via methylthiophene additive*. 2011. **1**(6): p. 1058-1061.
123. Lu, L. and L.J.A.M. Yu, *Understanding low bandgap polymer PTB7 and optimizing polymer solar cells based on it*. 2014. **26**(26): p. 4413-4430.
124. Yao, H., et al., *Molecular design of benzodithiophene-based organic photovoltaic materials*. 2016. **116**(12): p. 7397-7457.
125. Zhang, S., L. Ye, and J.J.A.E.M. Hou, *Breaking the 10% Efficiency Barrier in Organic Photovoltaics: Morphology and Device Optimization of Well-Known PBDTTT Polymers*. 2016. **6**(11): p. 1502529.
126. Pan, H., et al., *Low-temperature, solution-processed, high-mobility polymer semiconductors for thin-film transistors*. 2007. **129**(14): p. 4112-4113.
127. Hou, J., et al., *Bandgap and molecular energy level control of conjugated polymer photovoltaic materials based on benzo [1, 2-b: 4, 5-b'] dithiophene*. 2008. **41**(16): p. 6012-6018.
128. Huo, L. and J.J.P.C. Hou, *Benzo [1, 2-b: 4, 5-b'] dithiophene-based conjugated polymers: band gap and energy level control and their application in polymer solar cells*. 2011. **2**(11): p. 2453-2461.
129. Li, Y.J.A.o.c.r., *Molecular design of photovoltaic materials for polymer solar cells: toward suitable electronic energy levels and broad absorption*. 2012. **45**(5): p. 723-733.

130. Reddy, S.S., et al., *A new benzodithiophene based donor-acceptor  $\pi$ -conjugated polymer for organic solar cells*. 2020. **28**: p. 179-183.
131. Huang, P., et al., *Benzodifuran and benzodithiophene donor-acceptor polymers for bulk heterojunction solar cells*. 2015. **3**(13): p. 6980-6989.
132. Peet, J., et al., *Efficiency enhancement in low-bandgap polymer solar cells by processing with alkane dithiols*. 2007. **6**(7): p. 497-500.
133. Li, Z., et al., *Alternating copolymers of dithienyl-s-tetrazine and cyclopentadithiophene for organic photovoltaic applications*. 2011. **23**(7): p. 1977-1984.
134. Albrecht, S., et al., *Fluorinated copolymer PCPDTBT with enhanced open-circuit voltage and reduced recombination for highly efficient polymer solar cells*. 2012. **134**(36): p. 14932-14944.
135. Zhu, Z., et al., *Panchromatic conjugated polymers containing alternating donor/acceptor units for photovoltaic applications*. 2007. **40**(6): p. 1981-1986.
136. Moulé, A.J., et al., *Two novel cyclopentadithiophene-based alternating copolymers as potential donor components for high-efficiency bulk-heterojunction-type solar cells*. 2008. **20**(12): p. 4045-4050.
137. Osaka, I., et al., *Naphthodithiophene-based donor-acceptor polymers: versatile semiconductors for OFETs and OPVs*. 2012. **1**(4): p. 437-440.
138. Steinberger, S., et al., *ADADA-type oligothiophenes for vacuum-deposited organic solar cells*. 2011. **13**(1): p. 90-93.
139. Yang, M., et al., *A solution-processable D-A-D small molecule based on isoindigo for organic solar cells*. 2013. **48**: p. 1014-1020.

140. Zhang, J., et al., *Triphenylamine-containing D–A–D molecules with (dicyanomethylene) pyran as an acceptor unit for bulk-heterojunction organic solar cells*. 2011. **21**(11): p. 3768-3774.
141. Yassin, A., et al., *Donor–acceptor–donor (D–A–D) molecules based on isoindigo as active material for organic solar cells*. 2013. **37**(2): p. 502-507.
142. Schlick, T., *Molecular modeling and simulation: an interdisciplinary guide*. Vol. 2. 2010: Springer.
143. Mortuza, S., et al. *Molecular modeling of nanoparticles and conjugated polymers during synthesis of photoactive layers of organic photovoltaic solar cells*. in *2013 AIChE Annual Meeting*. 2013.
144. Dubbeldam, D., et al., *Highlights of (bio-) chemical tools and visualization software for computational science*. 2019. **23**: p. 1-13.
145. Dennington, R., T.A. Keith, and J.M.J.S.I.S.M. Millam, KS, USA, *GaussView 6.0*. 16. 2016: p. 143-150.
146. Radom, L.J.N., *John A. Pople (1925–2004)*. 2004. **428**(6985): p. 816-816.
147. Frisch, A.J.W., USA, 25p, *gaussian 09W Reference*. 2009. **470**.
148. Ramachandran, K., D. Gopakumar, and K. Namboori, *Basis sets*. 2008: Springer.
149. Elangovan, N., et al., *Synthesis, Spectral analysis, XRD, Hirshfeld surface analysis, DFT studies and Anticancer activities of di (o-chlorobenzyl)(dichloro)(1, 10-phenanthroline) tin (IV) complex*.
150. Schaftenaar, G., E. Vlieg, and G.J.J.o.c.-a.m.d. Vriend, *Molden 2.0: quantum chemistry meets proteins*. 2017. **31**: p. 789-800.

151. Samet, A., et al., *Optical properties and ab initio study on the hybrid organic–inorganic material [(CH<sub>3</sub>)<sub>2</sub>NH<sub>2</sub>]<sub>3</sub>[BiI<sub>6</sub>]*. 2010. **977**(1-3): p. 72-77.
152. Tirado-Rives, J., W.L.J.J.o.c.t. Jorgensen, and computation, *Performance of B3LYP density functional methods for a large set of organic molecules*. 2008. **4**(2): p. 297-306.
153. Tsipis, A.C.J.C.C.R., *RETRACTED: DFT flavor of coordination chemistry*. 2014. **272**: p. 1-29.
154. Boese, A.D., J.M. Martin, and N.C.J.T.J.o.c.p. Handy, *The role of the basis set: Assessing density functional theory*. 2003. **119**(6): p. 3005-3014.

